ELECTROSTATIC INTERACTIONS AMONG HYDROPHOBIC IONS IN LIPID BILAYER MEMBRANES

O. S. ANDERSEN, *Department of Physiology and Biophysics, Cornell University Medical College, New York 10021,*
S. FELDBERG AND H. NAKADOMARI, *Division of Molecular Science, Department of Energy and Environment, Brookhaven National Laboratory, Brookhaven, New York 11973,*
S. LEVY AND S. MCLAUGHLIN, *Department of Physiology and Biophysics, State University of New York at Stony Brook, Stony Brook, New York 11790 U.S.A.*

ABSTRACT We have shown that the absorption of tetraphenylborate into black lipid membranes formed from either bacterial phosphatidylethanolamine or glycerolmonooleate produces concentration-dependent changes in the electrostatic potential between the membrane interior and the bulk aqueous phases.

These potential changes were studied by a variety of techniques: voltage clamp, charge pulse, and "probe" measurements on black lipid membranes; electrophroetic mobility measurements on phospholipid vesicles; and surface potential measurements on phospholipid monolayers. The magnitude of the potential changes indicates that tetraphenylborate absorbs into a region of the membrane with a low dielectric constant, where it produces substantial boundary potentials, as first suggested by Markin et al. (1971). Many features of our data can be explained by a simple three-capacitor model, which we develop in a self-consistent manner. Some discrepancies between our data and the simple model suggest that discrete charge phenomena may be important within these thin membranes.

INTRODUCTION

It is now generally recognized that hydrophobic ions absorb strongly into a region of a bilayer membrane near the membrane solution interface, as was first suggested by Ketterer et al. (1971). Numerous studies have been made of the electrical properties of a bilayer exposed to the lipid soluble ions tetraphenylborate ($T\phi B^-$)[1] (Mueller and Rudin, 1967, 1969; Liberman and Topaly, 1968; LeBlanc, 1969; Ketterer et al., 1971; Grigor'ev et al., 1972; Haydon and Hladky, 1972; deLevie et al., 1974*b*; Andersen and Fuchs, 1975; Gavach and Sandeaux, 1975; Szabo, 1976; Benz et al., 1976) and dipicryl-

[1]Abbreviations used in this paper: ANS^-, 1,8-anilinonaphthalenesulfonate; BPE, bacterial phosphatidylethanolamine; DTFB, 5,6-dichloro-2-trifluoromethylbenzamidazole; FCCP, carbonylcyanide-*p*-trifluoromethoxylphenylhydrazine; GMO, glycerylmonooleate; SDS^-, sodium dodecylsulfate; $T\phi B^-$, tetraphenylborate anion; TNS^-, 2,6-toluidinylnaphthalenesulfonate.

amine (Mueller and Rudin, 1967, 1969; Ketterer et al., 1971; de Levie and Vukadin, 1975; Bruner, 1975; Benz et al., 1976). The behavior is well understood, at least at low concentrations (Ketterer et al. 1971; Andersen and Fuchs, 1975; Bruner, 1975; Benz and Läuger, 1977), where Ketterer's model predicts and experiments confirm that both the conductance and the number of absorbed hydrophobic ions increase linearly with the aqueous concentration, that the ions move between the two energy wells with a single time constant when a voltage is applied across the membrane, and that the voltage required to move a given fraction of absorbed ions from one potential energy well to the other is independent of concentration.

At higher concentrations, however, serious anomalies are observed. Neither the conductance nor the number of lipid soluble ions absorbed into the wells, for example, continues to increase linearly with the aqueous concentration. Attempts to explain these deviations from the simple model in terms of a buildup of space charge within the membrane, a limited number of binding sites, or a limited aqueous solubility of the ion are discussed critically by Haydon and Hladky (1972) and by Andersen et al. (1977). We demonstrate, furthermore, that as the concentration of lipid-soluble ions increases, the time-course of the current can no longer be described by a single exponential relaxation and that increasingly large potentials must be applied to the membrane to move a given fraction of charge between the two wells. We propose that these and other anomalies are all due to the absorption of charge and the concomitant production of electrostatic "boundary potentials" within the membrane, a phenomenon first discussed by Markin et al. (1971) and Liberman and Margulis (1974). We comment in the Discussion on the possible biological significance of these boundary potentials.

GLOSSARY OF TERMS

$A(\mathrm{mol}^{1/2}\mathrm{m}^{1/2}\mathrm{C}^{-1})$	See Eq. A4
$C_a(\mu\mathrm{F/cm}^2)$	Adsorption capacitance. Eqs. B13, B14.
$C_b(\mu\mathrm{F/cm}^2)$	Specific capacitance of outer region of bilayer. Appendix A.
$C_{dl}(\mu\mathrm{F/cm}^2)$	Specific capacitance of diffuse double layer. Appendix A.
$C_i(\mu\mathrm{F/cm}^2)$	Specific capacitance of inner region of a lipid bilayer.
$C_o(\mu\mathrm{F/cm}^2)$	Specific capacitance of outer region of a lipid bilayer.
$C_o^*(\mu\mathrm{F/cm}^2)$	Specific capacitance of outer region of a lipid monolayer.
$C_m(\mu\mathrm{F/cm}^2)$	Specific, geometric, membrane capacitance. Eq. 8.
$C_m^*(\mu\mathrm{F/cm}^2)$	Specific membrane capacitance measured at low voltage and low frequency, Eq. B12.
F(C/mol)	Faraday's constant: 96,497 C/mol.
$G(V,0)(\mathrm{S/cm}^2)$	Instantaneous specific membrane conductance.
$G(0,0)(\mathrm{S/cm}^2)$	Instantaneous conductance in the limit $V = 0$.
$I(V,0)(\mathrm{A/cm}^2)$	Instantaneous current.
K(cm)	The adsorption coefficient for a bilayer. See Eq. 31.
K^*(cm)	The adsorption coefficient for a monolayer. See Eq. E12.
N(molecules/mol)	Avogadro's number. 6.02×10^{23} molecules/mol.
P(cm/s)	Permeability coefficient.

$T(^\circ)$	Temperature, Kelvin.
$U(n)(J/cm^2)$	Potential energy of a two-dimensional hexagonal array of unit charges. See Eq. E6.
$V_D(V)$	Dipole potential.
$V_m(V)$	Membrane voltage.
$V_o', V_o''(V)$	Voltage across outer regions of bilayer. See Eqs. 4 and 6.
$V_0(V)$	See Eq. 32.
$V_\infty(V)$	Magnitude of the monolayer macropotential. See Eq. E3.
$V_m(0)(V)$	Membrane voltage (during charge pulse experiment), just after charge injection. See Eq. 23.
$V_m(\infty)(V)$	Membrane voltage (during charge pulse experiment) after completion of ion translocation.
$\Delta V_m(V)$	See Eq. 24.
$\Delta V_{m,max}(V)$	See Eq. 25.
$\Delta v(V)$	Change in electrostatic potential in the middle of the membrane effected by adsorbed $T\phi B^-$.
$\Delta V(T\phi B^-)(V)$	Monolayer surface potential, measured in presence of $T\phi B^-$.
$\Delta(\Delta V)(V)$	$\Delta(\Delta V) = \Delta V(T\phi B^-) - \Delta V$
b(dimensionless)	See Eq. 10.
d(cm)	Membrane thickness. See Fig. 1 *d*.
e(C)	Electronic charge: 1.6021×10^{-19} C.
g(S cm/mol)	See Eq. 36.
$i_c(A/cm^2)$	Current flow in external circuit per unit area of bilayer membrane.
$k(J/^\circ)$	Boltzmann's constant.
$n(molecules/cm^2)$	Number of adsorbed $T\phi B^-$ ions per square centimeter.
$q^0(C/cm^2)$	Charge density of counter ions of adsorbed $T\phi B^-$ on each side of the bilayer membrane.
$q_c(C/cm^2)$	Charge moved in external circuit per unit area of bilayer membrane.
$q', q''(C/cm^2)$	Magnitude of adsorbed charge density of $T\phi B^-$ on left and right sides of bilayer membrane.
$\Delta q(C/cm^2)$	See Eq. 17.
$\Delta q_c(C/cm^2)$	See Eq. 22.
$x(cm)$	Distance parameter normal to the plane of the membrane.
$\phi(V)$	Magnitude of the boundary potential within the membrane.
$\Phi(V)$	Micropotential. See Eq. E3.
$\psi(V)$	Diffuse double layer potential.
$\alpha(V^{-1/2})$	See Eq. E 11.
β(dimensionless)	See Eq. B 6.
δ(cm)	Locus of plane of adsorbed ions in a bilayer membrane. See Fig. 1 *d*.
δ^*(cm)	Locus of plane of adsorbed ions in a monolayer. See Eq. E8.
$\epsilon_0(F/m)$	Permitivity of free space: $8.85 \cdot 10^{-12}$ F/m.
$\epsilon_r^{aq}, \epsilon_r^{inner}$(dimensionless)	Relative dielectric constants for water, inner and outer regions of the bilayer membrane, and outer region of monolayer.
$\epsilon_r^{outer}, \epsilon_r^*$	
$\kappa(cm^{-1})$	Reciprocal Debye length. See Eq. A10 and Fig 1 *d*.
κ_T(dimensionless)	Lattice constant (see Eq. E7); 9.03 for a square lattice and 8.89 for a hexagonal lattice.
μ(C-cm)	Dipole moment.
τ, τ_1, τ_2(s)	Time constant for exponential decay curve.

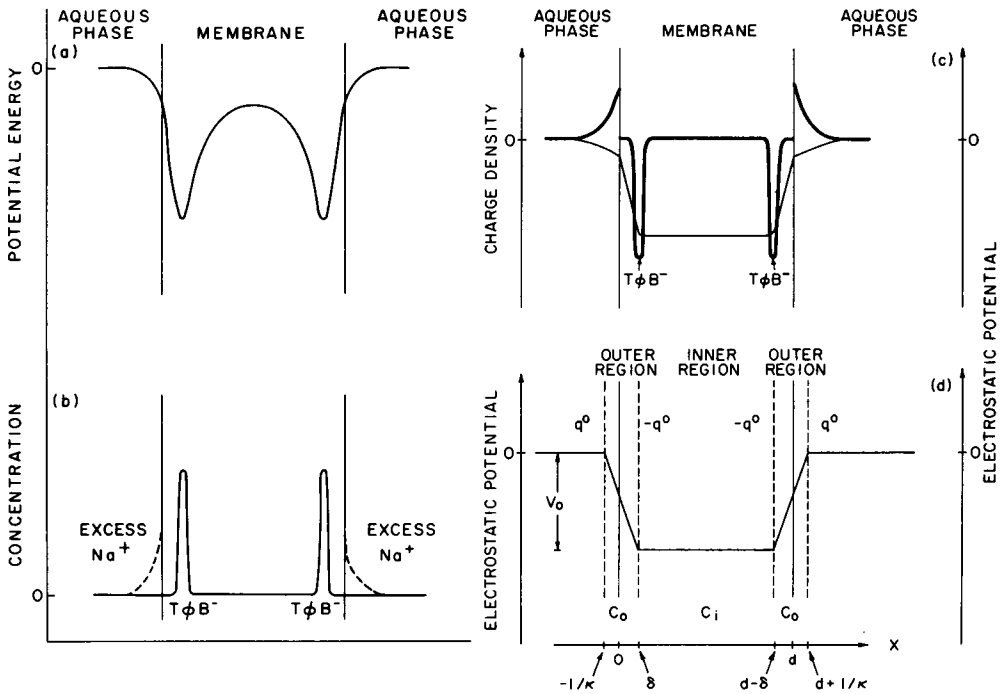

FIGURE 1 Schematic representation of the three-capacitor model. (*a*) The potential energy profile experienced by a single $T\phi B^-$ ion as it crosses a lipid bilayer membrane. We assume, for simplicity, that no interfacial barrier exists. (*b*) The concentration profiles for $T\phi B^-$ and Na^+, measured with respect to their concentrations in the bulk aqueous phases. (*c*) The charge distribution (heavy lines) and electrostatic potential profile (light lines) in the membrane and aqueous diffuse double layers. (*d*) The three-capacitor model for the electrostatic potential. The loci of the adsorbed $T\phi B^-$ ions (δ, $d - \delta$) and aqueous counterions ($-1/\kappa$, $d + 1/\kappa$) define four planes and three regions of the membrane. These regions can be regarded as three capacitors. See text for details.

THEORY

Model

A black lipid membrane extending from $x = 0$ to $x = d$ is assumed to be located between two symmetrical aqueous phases which contain equal concentrations of the hydrophobic anion tetraphenylborate, $T\phi B^-$. The aqueous phases contain a large excess of inert electrolyte which minimizes, but does not eliminate, the aqueous diffuse double-layer potentials due to the absorption of $T\phi B^{-1}$ into the membrane. As discussed in more detail by Ketterer et al. (1971), Läuger and Neumcke (1973), and Andersen and Fuchs (1975), chemical (mainly hydrophobic) and electrostatic (mainly pre-existing dipole potential and induced ion-dipole or image charge potentials) potential energies combine to establish deep potential energy wells for a $T\phi B^-$ ion near the membrane solution interfaces (Fig. 1 *a*). $T\phi B^-$ ions partition into the wells while their counterions, Na^+, remain behind, forming a diffuse double layer in each

aqueous phase (Fig. 1 *b*). This charge separation changes the electrostatic potential difference between the bulk aqueous phases and the planes of adsorbed charge.[2]

The adsorption of $T\phi B^-$ produces a change in the electrostatic potential between the bulk aqueous phase and the membrane solution interface (see Fig. 1 *c*). If the adsorbed anions are located within the low dielectric constant interior of the membrane, an additional change in potential will be produced within the membrane (see Fig. 1 *c*). We assume for simplicity that the adsorbed charges are smeared uniformly[3] over planes located at $x = \delta$ and $x = d - \delta$. As discussed in more detail in Appendix A, the counterions may be considered to be located in two planes at $x = -1/\kappa$ and $x = d + 1/\kappa$, where $1/\kappa$ is the Debye length (Fig. 1 *d*). We have thus defined four planes of charge and three dielectric regions: an outer region between $-1/\kappa$ and δ, with an effective dielectric constant $\epsilon_r^{\text{outer}}$ (defined by Eq. A12), an inner region between δ and $d - \delta$ with an effective dielectric constant $\epsilon_r^{\text{inner}}$ (probably close to 2), and an outer region between $d - \delta$ and $d + 1/\kappa$ with an effective dielectric constant $\epsilon_r^{\text{outer}}$. The specific capacitances of the outer regions are therefore: $C_o = \epsilon_r^{\text{outer}}\epsilon_0/(\delta + 1/\kappa)$, and the specific capacitance of the inner region is $C_i = \epsilon_r^{\text{inner}}\epsilon_0/(d - 2\delta)$. The adsorbed $T\phi B^-$ ions produce changes in the electrical potentials across these regions. We define these changes in electrostatic potential as the outer potentials, V_o' and V_o'', and the inner potential, V_i, (see also Fig. 2 *a*). When no potential is applied across a membrane in equilibrium with the symmetrical aqueous phases, the outer potential on the left side of the membrane is (setting the potential of the left bulk aqueous phase equal to zero):

$$V_o' = -q'/C_o = -q^0/C_o, \tag{1}$$

and the outer potential on the right side of the membrane is:

$$V_o'' = q''/C_o = q^0/C_o, \tag{2}$$

where q' and q'' are the magnitudes of the adsorbed charge density in the left- and right-hand wells, respectively, and q^0 is the magnitude of the adsorbed charge density in either well at equilibrium. (We shall, in the derivation of all subsequent equations, assume that the adsorbed species is an anion).

We assume that there is no ion transport across the outer regions once adsorption equilibrium is attained (e.g. Ketterer et al. 1971; Haydon and Hladky, 1972, Andersen

[2]We use the word adsorption rather than absorption because we assume that the ions are located in a plane, even though we believe that this plane is located within the membrane rather than at the membrane-solution interface. Although a dipole potential exists at each membrane solution interface, it is not explicitly represented in our schematic drawings. In subsequent discussion we define V_o' and V_o'' as the *change* in potential across the outer region effected by charge adsorption and/or by charge injection into the aqueous double layers. Thus, the value of the dipole potential is assumed constant and does not appear explicitly in any of our mathematical expressions.

[3]This assumption leads to a drastic simplification of the mathematical development of the model. It retains, however, the most important physical phenomenon: namely, that electrostatic potential changes are produced by adsorption of ions into the membrane phase. Some of the consequences of relaxing this assumption will be considered in Discussion section 3 and Appendix E.

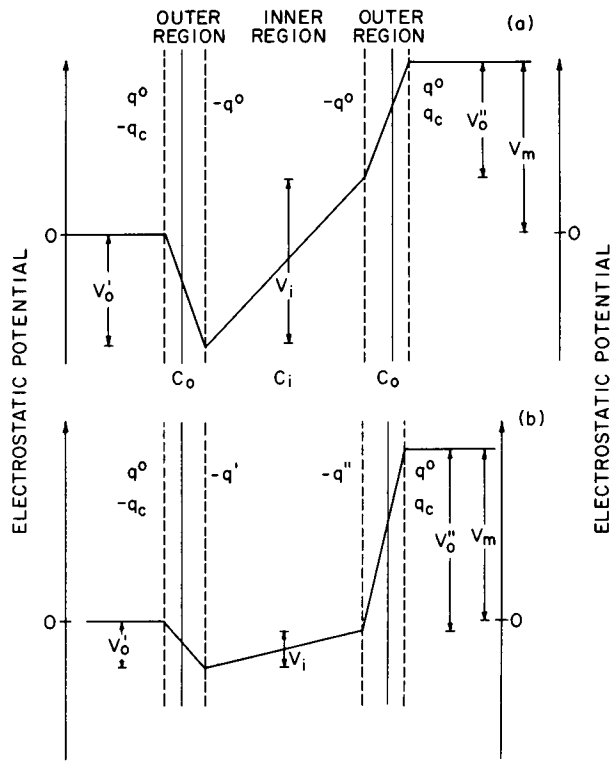

FIGURE 2 (*a*) Schematic representation of the potential profile after a potential difference, V_m, has been applied across the membrane but before any charge translocation has occurred. (*b*) Schematic representation of the potential profile across a lipid bilayer after some charge translocation has occurred. Note that the field in the membrane interior is now less than in Fig. 2*a*.

and Fuchs, 1975). The total amount of charge adsorbed in the membrane, $q' + q''$, is, therefore, independent of the applied potential and the resulting intramembrane charge translocation:

$$q' + q'' = 2q^0. \tag{3}$$

The application of a potential, V_m, (Fig. 2) or, equivalently, the injection of charge or passage of current through nonpolarizable electrodes in the aqueous phases introduces additional charge, q_c, into the plane at $x = d + 1/\kappa$ (i.e. the aqueous double layer on the right side of the membrane) while it removes the same quantity of charge from the plane at $x = -1/\kappa$.

The situation immediately after the application of a potential is shown schematically in Fig. 2 *a*. The situation after some charge has moved within the membrane is shown in Fig. 2 *b*. Using Gauss' theorem, we express the potential change across each of the three regions as follows:

$$V_o' = (q_c - q^0)/C_o, \tag{4}$$

$$V_i = (q_c - q^0 + q')/C_i, \tag{5}$$

$$V_o'' = (q^0 + q_c)/C_o. \tag{6}$$

The total membrane potential, V_m, is the sum of these potential changes:

$$V_m = V_o' + V_i + V_o'' = q_c \cdot (2/C_o + 1/C_i) + (q' - q^0)/C_i. \tag{7}$$

We define C_m as the specific membrane capacitance: it is measured either before any charge translocation has occured (i.e. $q' = q'' = q^0$) or in the limit of zero absorbed charge ($q^0 \rightarrow 0$). In other words:

$$C_m = \left(\frac{q_c}{V_m}\right)_{\substack{q'=q''=q^0 \\ \text{or } q^0=0.}} \tag{8}$$

Thus, from Eqs. 7 and 8 we deduce that:

$$1/C_m = 2/C_o + 1/C_i, \tag{9}$$

which illustrates that C_m is simply the series combination of the two outer capacitors and the inner capacitor.

It is convenient to define a term b as:

$$b = C_m/C_i. \tag{10}$$

Note that b is the fraction of the total membrane potential which falls across the inner membrane region either before any charge translocation has taken place ($q' = q'' = q^0$) or in the limit of zero adsorbed charge ($q^0 \rightarrow 0$). It is clear that:

$$0 \leq b < 1. \tag{11}$$

A value of $b = 0$ means that there is a single potential energy well in the middle of the membrane. When the ions are adsorbed to the membrane solution interface, the value of b approaches unity.[4]

Using Eqs. 9 and 10, we rewrite Eqs. 4–7 as:

$$V_o' = (1 - b) \cdot (q_c - q^0)/2C_m, \tag{12}$$

$$V_i = b \cdot (q_c + q' - q^0)/C_m, \tag{13}$$

$$V_o'' = (1 - b) \cdot (q_c + q^0)/2C_m, \tag{14}$$

$$V_m = [q_c + b \cdot (q' - q^0)]/C_m. \tag{15}$$

---

[4]We specify in our model (Appendix A) that the $T\phi B^-$ anions adsorb either within the membrane ($0 < \delta \leq d/2$ in Fig. 1*c*) or at the membrane solution interface ($\delta = 0$). In the latter case, b attains its maximum value. From Eqs. 10 and 11 we obtain quite generally that $b = 1 - 2C_m/C_o$. In the limit where the double-layer potential is small, and the $T\phi B^-$ anions are adsorbed at the membrane solution interface, one obtains from Eq. A11 that the outer capacitance, C_o, is equal to the capacitance of the diffuse double layer: $C_o = \kappa \cdot \epsilon_o \cdot \epsilon_r^{aq}$. To insert numerical values, the maximum value of b in a 1 M salt solution is about 0.995.

Combining Eqs. 13 and 15 gives:

$$V_i = b \cdot V_m - (1 - b) \cdot b \cdot \Delta q / C_m, \tag{16}$$

where

$$\Delta q = q^0 - q'. \tag{17}$$

Eq. 16 expresses the dependence of V_i, the potential between two energy wells (Fig. 2), upon V_m, the applied potential, and Δq, the amount of charge translocated from left to right within the membrane. Following the approach of Andersen and Fuchs (1975), we assume that at equilibrium the ratio of the charge densities in the two wells is given by the Boltzmann relation:

$$q''/q' = \exp\{e \cdot V_i/kT\}. \tag{18}$$

Analysis of Charge Movement in a Voltage-Clamp Experiment

When the membrane potential is changed from its initial value, zero, to a new value, V_m, one observes a current flowing in the external circuitry. With an idealized voltage clamp (zero external resistance, zero rise time, and infinite current output) one observes a delta function current transient which charges the membrane capacitance, C_m. This will be followed by a decaying current transient which results from ion translocation within the membrane (Ketterer et al., 1971; Andersen and Fuchs, 1975; Szabo, 1976). This external current arises because the value of q_c must change to keep V_m constant. At a given potential, V_m, we integrate the external current after the initial delta function transient to obtain the value of Δq_c where:

$$\Delta q_c = q_c - V_m \cdot C_m. \tag{19}$$

Since we have assumed that there is no ion translocation across the outer regions, it follows that Δq_c will reach an upper limit, $\Delta q_{c,\max}$, with increasing V_m. We assume that the final distribution of ions between the two wells is governed by the Boltzmann relation (see Eq. 18). In Appendix B we have expressed this relation in terms of measurable parameters:

$$\frac{\Delta q_{c,\max} + \Delta q_c}{\Delta q_{c,\max} - \Delta q_c} = \exp\left\{\frac{e}{kT} \cdot \left[b \cdot V_m - \frac{(1 - b) \cdot \Delta q_c}{C_m}\right]\right\}. \tag{20}$$

The relationship between the external charge moved, Δq_c, and the charge translocated within the membrane, Δq, is (see Eq. B 3).

$$\Delta q_c = b \cdot \Delta q = b \cdot (q^0 - q') = b \cdot (q'' - q^0), \tag{21}$$

from which it follows that:

$$\Delta q_{c,\max} = b \cdot q^0 \tag{22}$$

Eqs. 16, 18, and 20 are closely related to Eqs. 6, 9, and 10 of Andersen and Fuchs (1975). The two approaches become identical in the limit of $(1 - b) \cdot b \cdot q^0 \cdot e/(C_m \cdot$

$kT) = 0$. The important difference is that the present formalism can account for the dependence of V_i upon charge translocation within the membrane (Fig. 2; see also discussion in Appendix B). We believe that the present three-capacitor model constitutes the simplest possible extension of the treatment of Andersen and Fuchs (1975) that can account for the electrostatic potential changes associated with charge adsorption into, and charge movement within, lipid bilayer membranes.

Analysis of Charge Movement in a Charge Pulse Experiment

In a charge pulse experiment (Feldberg and Kissel, 1975), a known quantity of charge, q_c, is injected as quickly as possible (in zero time for the sake of the argument) into the aqueous solutions. The membrane potential is then observed at open circuit as a function of time. The initial membrane potential, $V_m(0)$, is measured just after charge injection but before any intramembrane charge translocation ($q' = q'' = q^0$). Therefore, (see Eq. 8):

$$V_m(0) = q_c/C_m. \tag{23}$$

The final voltage, $V_m(\infty)$, is reached when the translocation is complete, i.e. the value of q''/q' is determined by the Boltzmann relation (see Eq. 18). The difference between the initial and final membrane potential, ΔV_m, is proportional to the amount of charge translocated from one well to the other (Appendix C):

$$\Delta V_m = V_m(0) - V_m(\infty) = b(q^0 - q')/C_m. \tag{24}$$

The maximum value of ΔV_m is defined as $\Delta V_{m,\max}$ and is obtained in the limit where $V_m(\infty)$ is large enough to translocate all charge from one well to the other ($q' \to 0$):

$$\Delta V_{m,\max} = b \cdot q^0/C_m. \tag{25}$$

This leads directly (see Appendix C) to:

$$\Delta V_m = \Delta V_{m,\max} \tanh[(e/2kT)(b \cdot V_m(0) - \Delta V_m)]. \tag{26}$$

In a single pulse experiment it may be impossible to apply a sufficiently large pulse such that ΔV_m approaches $\Delta V_{m,\max}$. Even if $b = 1$, a potential $V_m(\infty) = 0.12$ V, is required to translocate 0.99 of the adsorbed charge from one well to the other (see Eq. 18). Thus, for ΔV_m to approach $\Delta V_{m,\max}$, we require that (see Eq. 24):

$$V_m(0) > 0.12 + q^0/C_m. \tag{27}$$

Few membranes are able to withstand more than 0.4 V without breaking. This limits a single pulse evaluation of $\Delta V_{m,\max}$ to conditions where $q^0/C_m < 0.3$ V, or inserting $C_m = 0.53\,\mu\text{F/cm}^2$ into Eq. 27, $q^0 < 1.5 \cdot 10^{-7}\,\text{C/cm}^2$. It is possible, however, to circumvent this limitation by using multiple charge injections to "pump" the translocation process to virtual completion.

The equation for analyzing any given pulse of a multiple pulse train is identical in form to Eq. 27. The voltage terms, however, must be redefined. Thus, for the j^{th} pulse:

$$V_m(0) = \sum_{n=1}^{j} (V_m(0))_n = \frac{1}{C_m} \sum_{n=1}^{j} (q_c)_n, \tag{28}$$

$$\Delta V_m = \sum_{n=1}^{j} (V_m(0))_n - (V_m(\infty))_n = \sum_{n=1}^{j} (\Delta V_m)_n, \tag{29}$$

and

$$\Delta V_{m,\max} = \sum_{n=1}^{\infty} (\Delta V_m)_n. \tag{30}$$

The voltages for the j^{th} pulse are measured with respect to base line for that pulse, in other words, versus $(V_m(\infty))_{j-1}$. The summation of an infinite number of pulses, Eq. 30, is clearly a mathematical idealization. In practice one sums over a number of pulses adequate to translocate virtually all the ions from one energy well to the other.

Analysis of Charge Adsorption as a Function of the Aqueous $[T\phi B^-]$

When a membrane is in equilibrium with the symmetrical aqueous solutions (in the absence of an applied potential), we assume that we can combine Henry's law and the Boltzmann relation to yield:

$$q^0 = F \cdot K \cdot [T\phi B^-] \cdot \exp\{-eV_o/kT\}, \tag{31}$$

where:

$$V_o = V_o'' = -V_o' = q^0/C_o, \tag{32}$$

and K, the adsorption coefficient, has the units of centimeters if q^0 is expressed in coulombs per square centimeter and $[T\phi B^-]$ is expressed in moles per cubic centimeter. (For a discussion of adsorption isotherms, the Gibbsian surface and the combination of Henry's law and the Boltzmann relation see Chapter 1 and Eq. 2.46 of Aveyard and Haydon (1973). We interpret K in the following manner: each boundary region of a membrane of area S contains, at equilibrium, the same number of adsorbed $T\phi B^-$ anions as does the aqueous phase of volume $K \cdot S$.

A combination of Eqs. 31 and 32 gives the following implicit equation for q^0 as a function of $[T\phi B^-]$:

$$q^0 = F \cdot K \cdot [T\phi B^-] \cdot \exp\{-eq^0/kTC_0\}. \tag{33}$$

The experimentally measurable parameters, however, are $\Delta q_{c,\max}$ and C_m, not q^0 and C_0. By substituting Eqs. 9, 10, and 22 into 33, one obtains:

$$\Delta q_{c,\max} = F \cdot b \cdot K [T\phi B^-] \exp\{-e(1-b) \cdot \Delta q_{c,\max}/2 \cdot b \cdot C_m \cdot kT\}. \tag{34}$$

METHODS AND MATERIALS

Planar black lipid membranes were formed at room temperature (22–25°C) across a hole, 1–1.6 mm^2 area, in a Teflon partition separating two Teflon chambers containing 1.0 M NaCl + 0.1 M phosphate buffered to pH = 7.3. The membranes were formed by the brush technique of

Mueller et al. (1963) or by the pipette technique of Szabo et al. (1969). The membrane-forming solutions were either bacterial phosphatidylethanolamine in *n*-decane, 2.5% wt/vol (BPE), or glycerolmonooleate dissolved in *n*-decane, 10% wt/vol (GMO).

After the BPE membrane was formed, the aqueous phases were stirred for 30 min before the voltage clamp experiments began. The experiments were initiated by adding a small portion of an ethanolic stock solution of NaTϕB to both aqueous phases. The adsorption of TϕB$^-$ into the bilayer reached equilibrium after about 15 min, at which time the electrical measurements were performed as rapidly as possible. At the end of the measurements a new aliquot of TϕB$^-$ was added, and so forth. For the charge pulse experiments the membranes were formed in solutions containing TϕB$^-$. The concentration of ethanol never exceeded 0.5% vol/vol, a concentration which has no effect on the observed phenomena.

The protocol for experiments with GMO membranes differed from the above due to poor membrane stability. The membranes were often formed in the presence of TϕB$^-$ and the measurements were generally done 5–10 min after the membrane had formed. (This short equilibrium period is permissible because the adsorption coefficient, K, is less for TϕB$^-$ into GMO than BPE bilayers).

Voltage-clamp experiments were done with a conventional two-electrode circuit. Membrane currents were measured in two ways. One method used a fast-settling, high slew-rate, differential amplifier (AD48, Analog Devices, Inc., Norwood, Mass.) in the virtual ground mode. To minimize overloading of the amplifier and oscilloscope, a limiting filter was inserted into the feedback loop (Andersen and Fuchs, 1975, Sargent, 1976). The signal from the function generator (F52A, IEC Corporation, Austin, Tex.) was fed through a unity gain voltage follower. Alternatively, the voltage drop across an external series resistor (100–1,000 Ω) was measured with a Tektronix 7623A oscilloscope equipped with a 7A22 differential amplifier (Tektronix, Inc., Beaverton, Ore.). The voltage pulses were produced by a low noise (model 164, Wavetek, San Diego, Calif.) pulse generator. Approaches 1 and 2 gave us identical results within experimental error. The performance of electrical systems was checked using an appropriate equivalent circuit (Ketterer et al., 1971). The response of the circuit to a voltage pulse was obtained by solving the second-order differential equation directly (Andersen, in preparation) or by Laplace transform methods (J. Dilger, personal communication, 1976). Great care was taken to minimize artifacts due to the finite rise of V_m (Andersen, in preparation). The electrodes were Ag/AgCl with a surface area of 2.5 cm^2. The total membrane capacitance was about 6 nF, the specific capacitance of BPE bilayers being 0.53 ± 0.01 μF/cm^2 and the specific capacitance of the GMO bilayers[5] being 0.47 ± 0.02 μF/cm^2. The time-course of the current transients and the determination of charge movement has been described previously (Andersen and Fuchs, 1975). At low concentrations of TϕB, the correlation coefficients of the current vs. time log-linear regressions were always better than −0.999. The initial current, $I(V, 0)$, was determined by extrapolating the regression line back to $t = 0$. The instantaneous conductance, $G(V, 0)$ is defined as:

$$G(V, 0) = I(V, 0)/V_m, \tag{35}$$

where V_m is the applied potential. Since the current-voltage characteristics were linear (within 6%) up to $V_m = 40$ mV, the instantaneous conductance in the limit of 0 mV applied potential, $G(0, 0)$ was approximated by $G(20, 0)$. The time constants of the current relaxations were also determined at 20 mV. They were identical, within experimental error, when determined as

[5]This value is higher than the value of 0.39 μF/cm^2 cited by Hladky and Haydon (1973) because the concentration of GMO in their membrane forming solution was 0.25% wt/vol. As expected, we found that membranes formed from solutions containing intermediate concentrations of GMO gave intermediate values for the specific capacitance.

described by Andersen and Fuchs (1975) from either the on or the off response. At high [TϕB$^-$] and, therefore, high q^0, the TϕB$^-$-induced current transients were definitely nonexponential (see, for example, Andersen et al., 1977), but only moderate errors (<10% at 10^{-6}M [TϕB$^-$]) in charge determination were introduced by approximating the current transients by a single exponential. The maximal charge translocated, $\Delta Q_{c,\max}$, and b were determined with a least-squares fit of the observed Δq_c vs. V_m data to Eq. 20. We thus determined both $\Delta q_{c,\max}$ and b. In some cases (where membrane stability was poor) $\Delta q_{c,\max}$ was approximated by the values of Δq_c obtained at high applied potentials.

Charge-pulse experiments used a multiple-pulse technique. The instrumentation was the same as that described by Feldberg and Nakadomari (1977). Data, recorded on the Nicolet 1093 digital oscilloscope (Nicolet Instrument Corp., Madison, Wis.), were analyzed by a least squares fit of the observed ΔV_m and $\Delta V_m(0)$ to Eq. 26. We thus determined both $\Delta V_{m,\max}$ and b; $\Delta q_{c,\max}$ was calculated with Eqs. 22 and 25.

Probe measurements were performed as described by McLaughlin and Harary (1976). Microelectrophoresis measurements were performed with a commercially available apparatus (Rank Bros., Bottisham, England) on phospholipid vesicles in 0.1 M and 1.0 M NaCl (buffered to pH 7.3 with phosphate) by the technique of Bangham et al. (1974). The Helmholtz-Smoluchowski equation was used to calculate the zeta potential from the mobility (e.g. Overbeek and Wiersema, 1967; Shaw, 1970: Aveyard and Haydon, 1973).

Surface potentials of monolayers at the air-solution interface were measured by the method of MacDonald and Bangham (1972), as described by Andersen et al. (1976). The aqueous subphase contained 1.0 M NaCl + 0.1 M phosphate at pH 7.3 and was stirred continuously throughout the experiment. After the potential of the clean air-electrolyte interface was established, 5 μl of BPE-*n*-hexadecane (2.5% wt/vol) were spread on the interface. A new stable potential was established within 10 min. After an additional 10 min, an aliquot of NaTϕB in ethanol was added to the subphase. These concentrations of ethanol had no measurable effect on the surface potential (Andersen et al., 1976). A stable potential was again established within 10 min. Additional aliquots were then added and the potential measured after each addition.

BPE was obtained from Supelco, Inc. (Bellefonte, Pa.), GMO from Sigma Chemical Co. (St. Louis, Mo.), *n*-decane and *n*-hexadecane were obtained from E. Merck (Darmstadt, Germany, through E.M. Laboratories, Inc., Elmsford, N.Y.) or from Supelco, Inc. NaTϕB (Kalignost) was obtained from E. Merck (through E.M. Labs) or from Aldrich Chemical Co., Inc. (Milwaukee, Wis.), DTFB was synthesized by the method of Acheson et al. (1958), FCCP was obtained from Pierce Chemical Co. (Rockford, Ill.), and nonactin was a gift from Ms. B. Stearns of E.R. Squibb & Sons (Princeton, N.J.). Inorganic chemicals were analytical grade. The water was either doubly distilled, or high-purity deionized (Millipore Super "Q", Millipore Corp., Bedford, Mass.).

RESULTS

Charge Adsorption and Conductance as a Function of TϕB$^-$ Concentration

BPE MEMBRANES Eq. 34 shows that b can be determined by measuring $\Delta q_{c,\max}$ as a function of the aqueous TϕB$^-$ concentration. Such measurements are shown in Fig. 3*a*. The most accurate data are obtained for $10^{-8} \leq$ [TϕB$^-$] $\leq 10^{-6}$M. The solid curve is a log-log least-squares best fit of these data to Eq. 34. With the measured value of 0.53 μF/cm^2 for C_m, this analysis gives b = 0.985 and K = 0.037 cm.[6]

[6]The adsorption coefficient for TϕB$^-$ into BPE bilayers is one order of magnitude larger than the value deduced by Andersen and Fuchs (1975). We do not understand the origin of this difference.

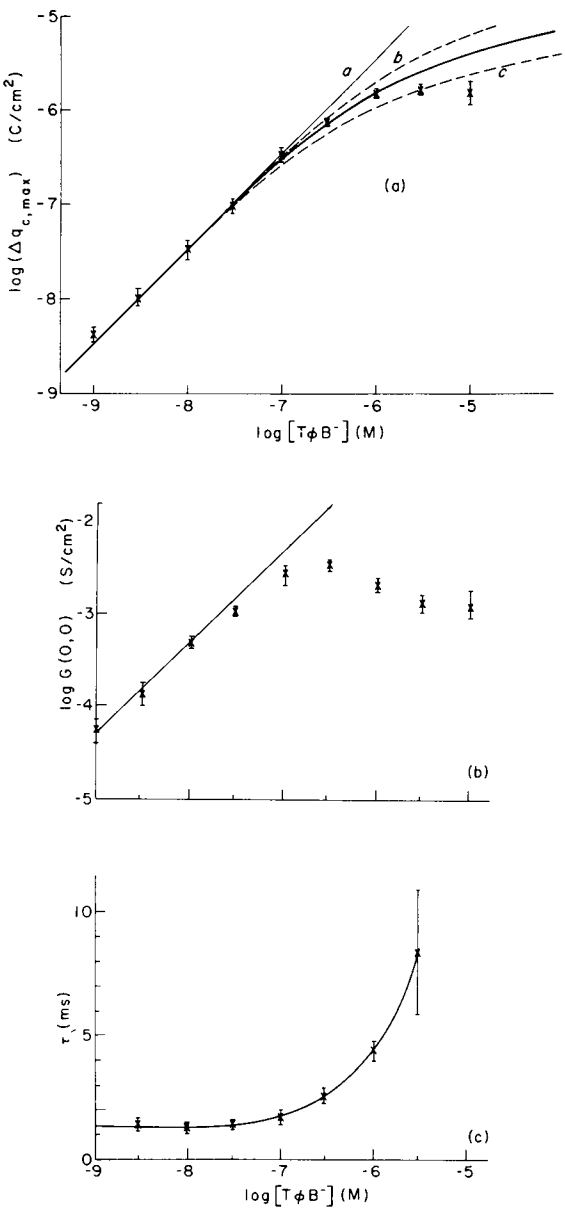

FIGURE 3 (*a*) A plot of $\Delta q_{c,\max}$ as a function of the aqueous tetraphenylborate concentration [$T\phi B^-$] for BPE bilayers. Each point indicates the mean (±SD) of measurements on at least five different membranes at each concentration. See text for details. (*b*) Membrane conductance, $G(0,0)$ as a function of [$T\phi B^-$]. The points indicate the mean (± SD) of measurements on at least six different membranes. The straight line illustrates the linear dependence of $G(0,0)$ on [$T\phi B^-$] observed at low concentrations. (*c*) Dependence of relaxation time constant on [$T\phi B^-$]. The points are the means (± SD). The line connecting the points has no theoretical significance.

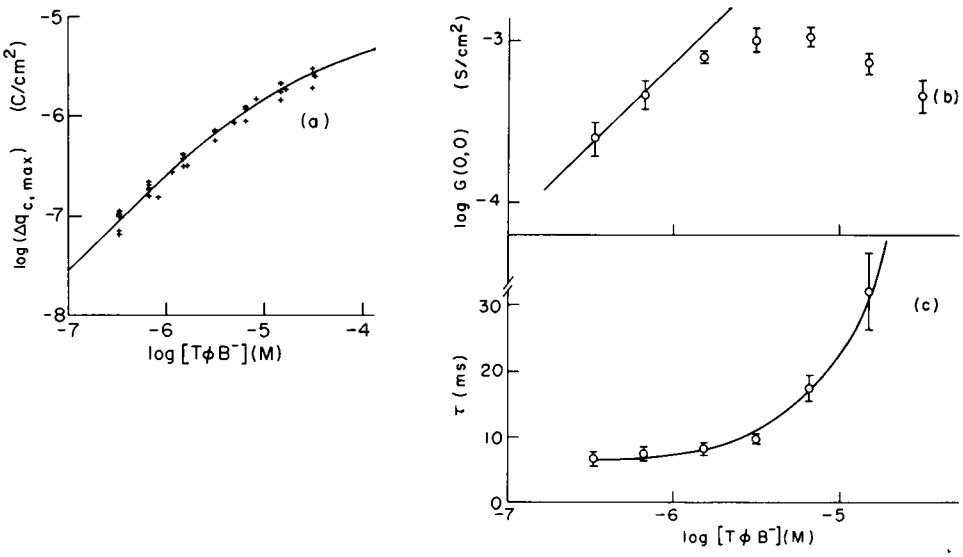

FIGURE 4 (*a*) Maximal transferred charge, $\Delta q_{c,\,max}$, as a function of $[T\phi B^-]$ for GMO membranes. Each point indicates a measurement on a different membrane. See text for details. (*b*) Membrane conductance, $G(0,0)$, as a function of $[T\phi B^-]$. The points indicate the means (± SD) of measurements on at least five different membranes. (*c*) Dependence of relaxation time constant on $[T\phi B^-]$. The points are the means (± SD). The line connecting the points has no theoretical significance.

From Eqs. 9 and 10 we deduce that $C_0 \simeq 70\ \mu F/cm^2$. For comparison we show three additional theoretical curves: a straight line, *a*, drawn according to Henry's law with $K = 0.037$ cm, curves *b* and *c* drawn for constant $b \cdot K$ and values of $C_0 = 140\ \mu F/cm^2$ ($b = 0.992$) and $35\ \mu F/cm^2$ ($b = 0.972$), respectively.

Fig. 3 *b* shows that the low potential instantaneous membrane conductance, $G(0,0)$ increases linearly with $[T\phi B^-]$ at low concentrations. The straight line has been drawn according to:

$$G(0,0) = g \cdot [T\phi B^-], \tag{36}$$

where $g = 5.0 \cdot 10^7$ S cm/mol. The fall in conductance we observe at $T\phi B^-$ concentrations above 3×10^{-7}M ($q^0 = 8 \cdot 10^{-7}$ C/cm², see Fig. 3 *a*) is similar to that observed by other investigators with $T\phi B^-$ (Andersen and Fuchs, 1975; Gavach and Sandeaux, 1975) and with dipicrylamine (Ketterer et al., 1971; Bruner, 1975; Gavach and Sandeaux, 1975). Neither this fall in conductance (Fig. 3 *b*) nor the associated increase in the relaxation time constant (Fig. 3 *c*) is predicted by the present three-capacitor model.[7]

GMO MEMBRANES Fig. 4 *a* shows the relationship between $\Delta q_{c,max}$ and

[7]At $[T\phi B^-] > 10^{-6}$M we observed additional complications. The membrane conductance shows an anomalous behavior during repeated electrical stimulation reminiscent of the observations of Ginsburg and Stark (1976) for picrate.

[TϕB$^-$] for GMO membranes. The solid curve is the log-log least-squares best fit of Eq. 34 to the data. Using the measured value of 0.47 μF/cm^2 for C_m, this analysis gives b = 0.99 and K = 0.0029 cm. From Eqs. 9 and 10 we deduce that $C_o \simeq 90$ μF/cm^2. Note that the value of K for GMO is an order of magnitude smaller than for BPE, while the values of C_o are similar.

Fig. 4 *b* shows that the conductance, $G(0,0)$ increases linearly with [TϕB$^-$] at low concentrations. The straight line is drawn according to Eq. 36 with $g = 7.6 \times 10^5$ S cm/mol. The decrease in conductance observed above 5×10^{-6} M TϕB$^-$ ($q^0 = 8 \times 10^{-7}$ C/cm^2, see Fig. 4 *a*) is again associated with an increase in the relaxation time constant, as seen in Fig. 4 *c*.

The Effect of TϕB$^-$ on the Boundary Potential

PROBE MEASUREMENTS The adsorption of TϕB$^-$ into BPE bilayers depresses the conductance due to the anion probe DTFB, as illustrated by the circles in Fig. 5. This depression is consistent with the adsorption of TϕB$^-$, producing a (negative) potential.

The change in electrostatic potential in the middle of the membrane, Δv, may be estimated from the expression (McLaughlin, 1977)

$$G^*_{DTFB}(0,0)/G_{DTFB}(0,0) = \exp\{e \cdot \Delta v/kT\}, \quad (37)$$

where $G_{DTFB}(0,0)$ and $G^*_{DTFB}(0,0)$ are the DTFB conductances in the absence and presence of TϕB$^-$, respectively. The right-hand ordinate of Fig. 5 illustrates the values

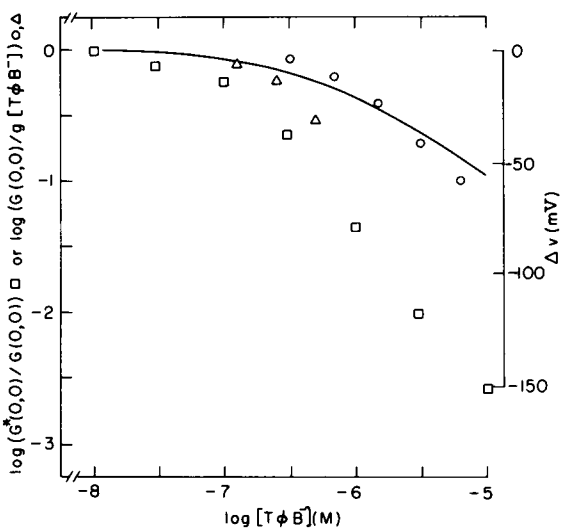

FIGURE 5 Use of probe measurements to estimate the change in electrostatic potential produced by TϕB$^-$ in bilayers formed from BPE. The left-hand ordinate indicates the normalized conductance produced by DTFB (circles), FCCP (triangles), and TϕB$^-$ (squares). These normalized conductances are defined by the left-hand sides of Eq. 37 and 39. The right-hand ordinate indicates the change in surface potential, Δv, calculated from Eqs. 37 or 39. The curve indicates the prediction of the three-capacitor model (Eq. 38).

of Δv calculated from Eq. 37. The solid line is the change in the electrostatic potential in the middle of the membrane, V_0, predicted by the three-capacitor model. This is calculated from a combination of Eqs. 32 and 33:

$$V_o = (FK/C_0) \cdot [T\phi B^-] \cdot \exp\{-e \cdot V_o/kT\}, \quad (38)$$

using the values of C_0 and K which gave the best fit to the data of Fig. 3 *a*.

We can also use the $T\phi B^-$ conductance to estimate Δv as a function of $[T\phi B^-]$. Eq. 36 and the obvious extension of Eq. 37 yield:

$$G(0,0)/(g \cdot [T\phi B^-]) = \exp\{e \cdot \Delta v/kT\}, \quad (39)$$

where $g = 5 \cdot 10^7$ S · cm/mol in BPE membranes. The values of Δv estimated from $T\phi B^-$ conductance measurements are shown by squares in Fig. 5.

Finally, the results obtained from the use of the anionic probe FCCP are indicated by triangles in Fig. 5. Note that the potential in the interior of the membrane estimated with the anionic probes tends to be more negative than the potential predicted by the three-capacitor model. Experiments with positive probes have uniformly shown larger conductance changes than observed with anionic probes. For example, we observe a 10-fold increase in nonactin-K^+ conductance at $[T\phi B^-] = 3 \cdot 10^{-7}$M. A quantitative interpretation of these conductance changes is, complicated, however, by specific interactions between $T\phi B^-$ and the cation probes (e.g. the measured $T\phi B^-$ adsorption decreases with increasing nonactin-K^+ concentration). Similar asymmetries in the responses of anionic and cationic probes have also been observed with picrate, which like $T\phi B^-$ and dipicrylamine produces large changes in boundary potentials (S. McLaughlin, unpublished).

ZETA POTENTIAL MEASUREMENTS Calculations based on the Gouy-Chapman theory of the diffuse double layer (e.g. McLaughlin, 1977) indicate that $2 \cdot 10^{-6}$M $T\phi B^-$ should cause negligible (< 10 mV) changes in the zeta potentials of BPE vesicles bathed in 1 M NaCl. This was confirmed by microelectrophoresis measurements of the mobility, u, in both 0.1 and 1 M NaCl, and calculations of the zeta potential, ζ, from the Helmholtz-Smoluchowski equation.

SURFACE POTENTIAL MEASUREMENTS Monolayers formed from BPE in hexadecane have a stable surface potential of 385 ± 8 mV, when well-defined lenses are present throughout the experiment. Addition of $T\phi B^-$ to the aqueous subphase causes potential changes. The potential changes are expressed as $\Delta(\Delta V) = \Delta V(T\phi B^-) - \Delta V$, where $\Delta V(T\phi B^-)$ and ΔV are the surface potentials measured in the presence and absence of $T\phi B^-$ with respect to the clean air-solution interface. In Fig. 6 we plot $\Delta(\Delta V)$ vs $[T\phi B^-]$. The dashed curve is drawn according to Eq. 38, with the same values of C_0 and K that gave the best fit in Fig. 3 *a*. The solid curves are predicted by a discrete charge model discussed in Appendix E. These results, obtained on BPE monolayers, are in qualitative agreement with those Babakov et al. (1972) obtained on mixed brain lipid monolayers, once it is recognized that these latter monolayers have a negative surface potential due to the presence of negatively charged lipids.

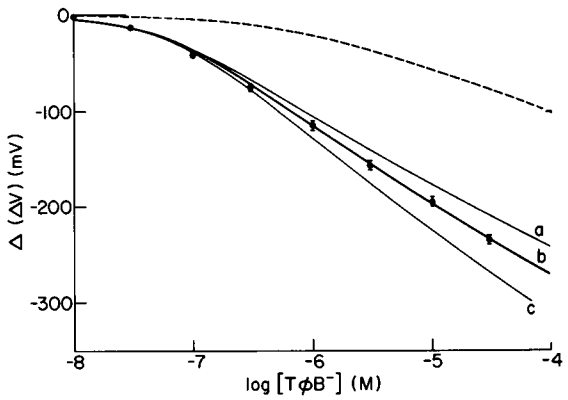

FIGURE 6 Changes in the surface potential, $\Delta(\Delta V)$, of BPE monolayers as a function of $[T\phi B^-]$. The dashed curve is drawn according to Eq. 38, with the values of C_o and K obtained from Fig. 3 *a*. The solid curves are calculated according to Eq. E13 with $K^*/C_o^* = 4.9\ 10^3$ Vcm^3/C and different values of α: (*a*) $\alpha = 1.134\ V^{-1/2}$; (*b*) $\alpha = 0.934\ V^{-1/2}$; (*c*) $\alpha = 0.734\ V^{-1/2}$.

Charge Movement as a Function of Potential

Fig. 7 shows typical data that illustrate the relationship between Δq_c, the charge which moves in the external circuit (Eq. 19), and V_m, the applied potential at different $[T\phi B^-]$. Recall (Eq. 21) that Δq_c is approximately equal to the charge translocated within the membrane. The solid lines are the least-squares best fits of the experimental data to

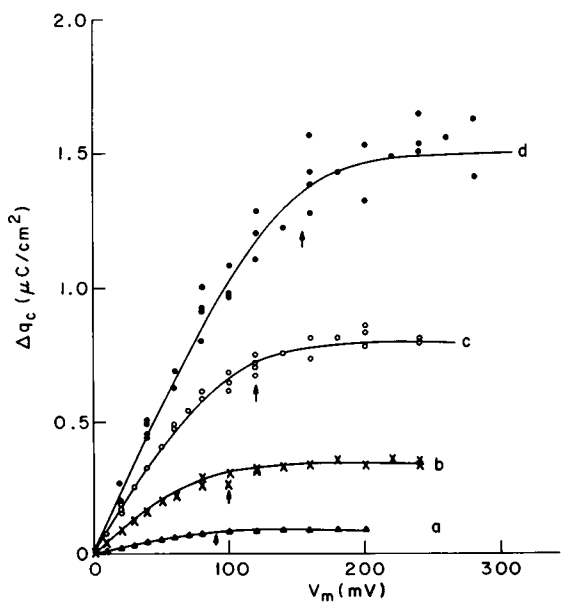

FIGURE 7 Plots of Δq_c vs. V_m at different $[T\phi B^-]$ for BPE membranes. The curves are the least square fits to Eq. 20. The arrows indicate the potentials required to translocate 90% of the adsorbed charge. (*a*, 3×10^{-8}M; *b*, 1×10^{-7}M; *c*, 3×10^{-7}M; *d*, 1×10^{-6}M).

TABLE I
VARIATION IN b WITH [TϕB$^-$]

[TϕB$^-$]	$\Delta q_{c,max}$	b	C_o	β
M	$\mu C/cm^2$		$\mu F/cm^2$	
1×10^{-8}	$3.5 \pm 0.8 \times 10^{-2}$	0.93 ± 0.03	15	0.86 ± 0.06
3×10^{-8}	$9.5 \pm 1.3 \times 10^{-2}$	0.95 ± 0.02	21	0.83 ± 0.05
1×10^{-7}	$3.5 \pm 0.6 \times 10^{-1}$	0.97 ± 0.01	35	0.71 ± 0.05
3×10^{-7}	$7.9 \pm 0.6 \times 10^{-1}$	0.971 ± 0.004	37	0.56 ± 0.04
1×10^{-6}	1.49 ± 0.13	0.971 ± 0.004	37	0.41 ± 0.05

The results are mean $\pm$ SD, and are averages of measurements on at least five BPE membranes at each concentration. $\Delta q_{c,max}$ and b are determined by a least-square fit to Eq. 34. β is determined by the procedure of Andersen and Fuchs (1975).

Eq. 20. The average values of b and $\Delta q_{c,max}$ determined in this manner are given in Table I. It should be apparent that our model predicts (Fig. 2) and experiments confirm (Fig. 7) that as the adsorbed charge density increases, increasingly large potentials must be applied to move a given fraction of charge from one well to another within the membrane. The arrows in Fig. 7 indicate the potentials required to move 90% of the charge. Table I illustrates that the present three-capacitor model is oversimplified because the values of b (or C_0) depend on [TϕB$^-$] (or $\Delta q_{c,max}$). Still, values of b obtained with the three-capacitor model are much more independent of [TϕB$^-$] than the values of β obtained from the model of Andersen and Fuchs (1975), which disregards boundary potentials (compare columns 3 and 5 in Table I).

Kinetics of Charge Movement at High [TϕB$^-$]

When an electrical potential difference, V_m, is applied across a membrane, charge moves between the two potential energy wells, changing the outer and inner potentials, as illustrated in Fig. 2. Our three-capacitor model predicts (Eq. B4 or 16 and 21) that the inner potential, V_i, decreases from an initial value of $b \cdot V_m$ to a final value of $b \cdot V_m - (1 - b) \cdot \Delta q_c/C_m$. As discussed in more detail by Feldberg and Delgado (1978), the current relaxations are not described by a single exponential when the applied potential, V_m, is large and the outer potentials, V_o' and V_o'', are significant.

At high [TϕB$^-$], we do find that a semilogarithmic plot of current vs. time exhibits nonlinear behavior (Fig. 8). The ratio of the initial and final slopes of this curve can be correlated with parameters of our model. The initial slope represents a hypothetical transient with a time constant τ_1, which would be observed if V_i were kept constant, equal to $b \cdot V_m$. The final slope represents a hypothetical transient with a time constant τ_2, which would be observed if V_i were kept constant equal to $b \cdot V_m - (1 - b) \cdot \Delta q_c/C_m$, where Δq_c is the equilibrium value. The experimental dependence of τ_1 on V_m was obtained from measurements at 10^{-8} M TϕB$^-$, where boundary potentials were assumed to be insignificant and $V_i = bV_m$ (data not shown). These measurements represent a calibration curve that allows us to deduce changes in V_i from τ_1 and τ_2.

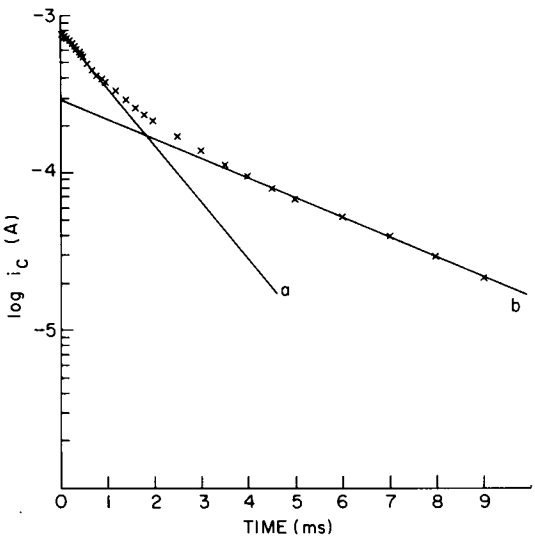

FIGURE 8 A semilogarithmic plot of current vs. time for a BPE membrane: $[T\phi B^-] = 10^{-6}$M, V_m = 160 mV. The initial slope (line *a*) represents a hypothetical transient with a time constant τ_1 = 1.2 ms, and the final slope (line *b*) represents a hypothetical transient with a time constant τ_2 = 3.4 ms.

Assuming that $b = 0.97$ and inserting the known values of C_m and Δq_c, we predict that when V_m = 160 mV and $[T\phi B^-] = 10^{-6}$M, the ratio of the two time constants should be 2.8, which corresponds with the average ratio of 2.8 ± 0.4 observed experimentally.

A similar test of the model is obtained from an analysis of the off-response. Immediately after the membrane potential is returned to zero, there exists a potential difference, $V_i = -(1 - b) \cdot \Delta q_c / C_m$ between the two potential energy minima. At the end of the off-response $V_i = 0$. The off-response will, therefore, also be nonexponential for large initial values of V_i. Using the same values of $b, \Delta q_c$, and C_m as above, we predict that when V_m = 160 mV and $[T\phi B^-] = 10^{-6}$M, the ratio of the final to the initial rate constant should be 2.0. This number agrees with the experimental values of 2.0 ± 0.4.

Charge-Pulse Measurements

Fig. 9 *a* shows a series of relaxations produced by a multiple charge pulse train across a BPE membrane ($[T\phi B^-] = 5.0 \times 10^{-8}$M). The first pulse (Fig. 9 *b*) produces a rapid initial rise in voltage, followed by a slow relaxation due to charge translocation in the membrane. The stable nonzero potential observed at the end of the relaxation supports the presumption that little or no charge is moving from one aqueous phase to the other through the membrane. As the charge is pumped from one well to the other, the magnitude of the relaxation diminishes, indicating that less charge remains to be

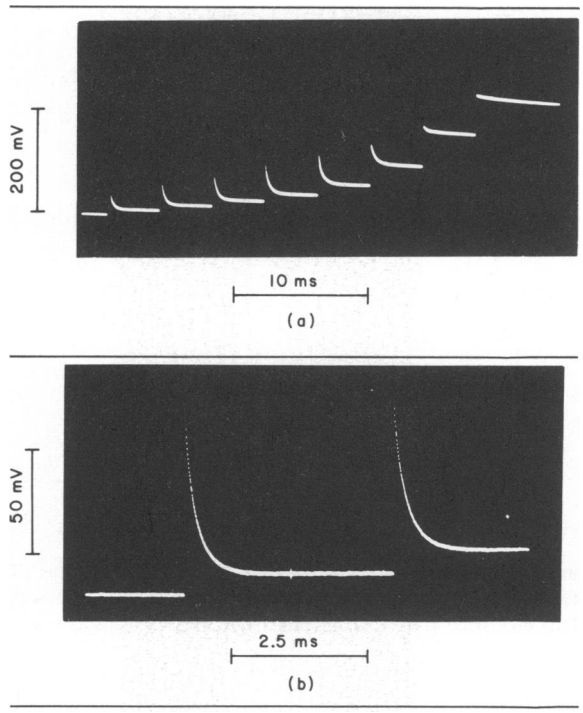

FIGURE 9 Multiple charge pulse experiment on a BPE membrane with $[T\phi B^-] = 5.0 \cdot 10^{-8}$M: (*a*) series of eight pulses, (*b*) expansion of first pulse. Details of the analysis are presented in the text.

translocated with each succeeding pulse. The final (right) pulse in Fig. 9*a*, exhibits virtually no fast relaxation.[8]

By using a least-squares fit and Eq. 26, these data were analyzed. For $[T\phi B^-] > 5 \cdot 10^{-8}$M, $b = 0.976 \pm 0.003$. This value of b is consistent with that obtained by the voltage clamp method (see Table I). The values of $\Delta q_{c,\max}$ deduced from the charge pulse data agree within experimental error with the voltage clamp data presented in Fig. 3*a*.

DISCUSSION

In section 1 we discuss our major experimental result, which is that the adsorption of $T\phi B^-$ into a phospholipid bilayer membrane changes the electrostatic profile across the membrane. In section 2 we discuss the location of $T\phi B^-$ within the membrane. In section 3 we discuss the ability of the three-capacitor model to describe our results, as well as the implications of the discrete nature of the adsorbed charges. In section 4 we discuss the possible biological significance of electrostatic boundary potentials.

[8]There is an indication of a slower relaxation at higher potentials. Similar relaxations have been observed by Benz et al. (1976). We compensate for this effect by extrapolating the slower voltage decay back to zero time (for that pulse) in order to evaluate $V_m(\infty)$.

1. *The Adsorption of $T\phi B^-$ Changes the Electrostatic Potential*

The significant deviations we observed from a Henry's law adsorption isotherm (Figs. 3*a* and 4*a*) are similar to those seen by other investigators for the lipid soluble anions $T\phi B^-$ (Grigor'ev et al., 1972; Benz et al., 1976) and dipicrylamine (Bruner, 1975; Benz et al., 1976; Wulf et al., 1977; Wang and Bruner, 1977). We also observed that the voltage required to translocate a given fraction of the adsorbed charge increased with $[T\phi B^-]$ (Fig. 7), and that the current transients became nonexponential at high $[T\phi B^-]$ when the applied potential, V_m, was large (Fig. 8). Although these observations are consistent with the three-capacitor model, they do not provide unequivocal evidence for a change in the electrostatic potential within the membrane. They could, for example, be due to the saturation of a limited number of binding sites for $T\phi B^-$ in the membrane (e.g. Ketterer et al., 1971)[9] or to some structural change in the membrane induced by $T\phi B^-$.

We have, however, more direct evidence that the adsorption of $T\phi B^-$ into BPE bilayers changes the electrostatic potential within the membrane. First, the adsorption of $T\phi B^-$ increases the conductance produced by positively charged probes (e.g. nonactin-K^+) and depresses the conductance produced by negatively charged probes (e.g. DTFB, FCCP, $T\phi B^-$). These observations imply that $T\phi B^-$ causes the electrostatic potential within the membrane to change in the negative direction. Second, the adsorption of $T\phi B^-$ into a BPE monolayer spread at the air-solution interface causes a substantial change of the surface potential in a negative direction. A similar potential change presumably occurs within the bilayer.

This change in potential cannot be explained merely by the production of an aqueous diffuse double layer because (*a*) the potential is much larger than that predicted by the Gouy-Chapman theory of the diffuse double layer and (*b*) no significant zeta potentials are observed. Most of the potential change thus occurs within the membrane phase. We interpret this change in potential as being due to adsorbed charges ($T\phi B^-$) within the membrane. We cannot, however, rule out the possibility that our observations are due to a change, induced by $T\phi B^-$, in the pre-existing dipole potential.

2. *The Location of $T\phi B^-$ within the Membrane*

Information about the location of $T\phi B^-$ within the bilayer may be obtained by comparing its adsorption into BPE and GMO membranes. The adsorption coefficient, K (Eq. 31), is about 10 times higher for BPE membranes (and also for dioleoyl

[9]One could analyze the present data in terms of a simple saturating binding model (Langmuir isotherm). A Scatchard plot (e.g. Edsall and Wyman, 1958) of the data in Fig. 3 *a* gives a reasonably straight line for $[T\phi B^-] \leq 10^{-6}$M. The predicted density of binding sites is $1/650\,\text{Å}^2$. A similar calculation yields a slightly higher density of binding sites for GMO bilayers. If one wished to take into account both electrostatic phenomena and a limited number of binding sites, the analysis can be made along the lines described by McLaughlin and Harary (1976). The electrostatic boundary potentials inferred from either probe measurements on bilayers or surface potential measurements on monolayers, however, are more than sufficient to explain the deviations from Henry's law observed in Fig. 3 *a*. It is, therefore, not necessary to invoke nonelectrostatic phenomena.

phosphatidylethanolamine membranes [O. Andersen, unpublished]) than for GMO membranes.

BPE bilayers have a larger (interior more positive) dipole potential than GMO bilayers (Hladky, 1974). By measuring the conductance produced by cations and anions, we estimate that the dipole potential in a BPE membrane is about 120 mV more positive than in a GMO membrane (Appendix D). If the observed 10-fold difference in adsorption coefficients were related only to the difference in the interfacial dipole potentials, and if the dipole potentials were not perturbed by $T\phi B^-$, we could conclude that a $T\phi B^-$ ion adsorbed into a BPE membrane experiences an electrostatic potential 60 mV more positive than a $T\phi B^-$ ion adsorbed into a GMO membrane. If we knew the location of the dipole(s), we could place an outer limit on the location of the $T\phi B^-$ adsorption plane. A reasonable guess (e.g. Paltauf et al., 1971; Haydon and and Hladky, 1972; McLaughlin, 1977; Benz and Läuger, 1977) is that the dipole potential originates in the glycerol backbone region and is associated with the three ester bonds.

Wang and Bruner (1977) have suggested that the value of C_o for the adsorption of dipicrylamine into phosphatidylcholine membranes is due entirely to a diffuse double-layer capacitance, C_{dl}. Specifically, they interpreted their adsorption data with a combination of Eqs. 33, A4, A5, and A6 with the assumption that $C_o = C_{dl}$. This interpretation led them to conclude that the dielectric constant of the aqueous phase adjacent to the membrane, $\epsilon_r^{\text{aqueous}}$, decreases from a value of 80 to 3 as the concentration of indifferent electrolyte increases from 10^{-4} to 1 M. Their experimental data are in agreement with ours: the potential changes are larger than can be explained by simple Gouy-Chapman theory. We believe their interpretation is incorrect for two reasons. First, in other studies where the Gouy equation from the theory of the diffuse double layer (Eq. A2) has been tested directly with measurements of both double layer potential and charge density (Haydon and Myers, 1973, McLaughlin and Harary, 1976), no evidence was found for saturation of the aqueous dielectric as a function of salt concentration. Second, at higher salt concentrations (10^{-1}M), the experimentally measured value of the zeta potential produced by 10^{-6}M dipicrylamine is much too low (< 10 mV, our measurements) to explain the observed deviation (one order of magnitude) from Henry's law (see also section 3*a*). We conclude, therefore, that the charge on the hydrophobic ion dipicrylamine is located deeper in the membrane than either the charge on the amphipathic ions SDS^- (Haydon and Myers, 1973) and TNS^- (McLaughlin and Harary, 1976) or the negative charge in the polar head group of a charged lipid (e.g. Benz and Läuger, 1977; McLaughlin, 1977).

3. *Limitations of the Three-Capacitor Model.*

a. CHARGE ADSORPTION AS A FUNCTION OF $[T\phi B^-]$ The experimentally observed relationship between charge adsorption into a BPE bilayer and $[T\phi B^-]$ is reasonably well described by the three-capacitor model (Fig. 3*a*) for $10^{-8} \leq [T\phi B^-] \leq 10^{-6}$ M, where we obtained the most accurate data. The origin of the

deviations observed for $[T\phi B^-] > 10^{-6}$M is unknown. The adsorption of dipicrylamine to bilayers formed from phosphatidylcholine, on the other hand, can be described quite accurately by the three-capacitor model (Fig. 20 in McLaughlin, 1977), even at high charge densities.

b. DEPENDENCE OF OUTER CAPACITANCE ON ADSORBED CHARGE The ability of the three-capacitor model to describe the Δq_c vs V_m curves of Fig. 7 is good, but not perfect. From Table I it is apparent that the value of b (or C_o) decreases when $[T\phi B^-] < 10^{-7}$M. This could be due to the discrete charge phenomena discussed in section *f* or to movement of the plane of adsorption towards the center of the membrane as $[T\phi B^-]$ decreases. Both interpretations are consistent with the observation that the normalized instantaneous conductance, $G(V,0)/G(0,0)$, increases more rapidly with voltage at high $[T\phi B^-]$ than at low $[T\phi B^-]$ (data not shown).

c. INCREASE OF τ WITH $[T\phi B^-]$ The increase of the relaxation time constant (Fig. 3*c* and 4*c*) is not predicted by the three-capacitor model. This increase is equivalent to the observation that $q^0/G(0,0)$ increases with increasing $[T\phi B^-]$. Andersen and Fuchs (1975) or Szabo (1976) may be consulted for a detailed discussion of why τ is proportional to $q^0/G(0,0)$ at low $[T\phi B^-]$. The increase in τ is therefore in qualitative agreement with the results obtained with probes (Fig. 5) and the results obtained from adsorption data (Fig. 3*a*), namely that the potential change near the middle of the membrane is larger than the potential change in the plane of adsorption. A similar conclusion was reached by Wulf et al. (1977). This difference in potentials could be due to the discrete charge phenomena discussed in section *f*.

d. PROBE MEASUREMENTS ON BILAYERS When the diffuse double-layer potential at the surface of a membrane is modified by changing either the ionic strength of the aqueous phase or the charge density at the membrane solution interface, one observes symmetrical effects with positive and negative probes (e.g. McLaughlin, et al., 1970, 1971; McLaughlin, 1973, 1975; McLaughlin and Harary, 1976). Symmetrical effects have also been observed with salicylamide (McLaughlin, 1973) and phloretin (Andersen et al., 1976), neutral molecules which change the dipole potential. When we used different ion probes to estimate the magnitude of the "boundary" potential produced by $T\phi B^-$, however, we observed quite asymmetrical results with positive and negative probes. For example, at $3 \cdot 10^{-7}$ M $T\phi B^-$, we estimated V_o to be -60 mV with the nonactin-K^+ probe but only -10 mV with the DTFB probe. This appears to be a general phenomenon when dealing with lipid-soluble ions which adsorb within the membrane and produce boundary potentials. Picrate, for example, at a concentration of 10^{-3} M, enhances the conductance of nonactin-K^+ or valinomycin-K^+ about 2.5 orders of magnitude but depresses the conductance of the negative probes DTFB and FCCP only about 0.5 orders of magnitude (S. McLaughlin, unpublished). At this concentration, picrate produces a zeta potential of only -20 mV, which indicates, in conjunction with the probe measurements, that it produces a large "boundary" potential. Other workers have observed analogous effects with hydrophobic ions (e.g. Liberman and Topaly, 1969, Hinkle, 1970). We suspect that this asymmetry is due in part to the discrete charge effects discussed in section *f*.

e. SURFACE POTENTIAL MEASUREMENTS ON MONOLAYERS The three-capacitor model fails to account for the changes in the surface potentials of monolayers greater than 2.3 kT/e per decade of $[T\phi B^-]$ (see Fig. 6), which is the maximum slope predicted by either a three-capacitor or Gouy-Chapman model (Appendix E). The change in surface potential with $[T\phi B^-]$, $\partial\Delta(\Delta V)/\partial \log\{[T\phi B^-]\}$, is the Esin-Markov coefficient and a coefficient greater in magnitude than 2.3 kT/e has traditionally been ascribed to discrete charge effects (e.g., Grahame, 1958; Barlow and Macdonald, 1967). If we assume that the adsorption coefficient of $T\phi B^-$ into BPE monolayers is the same as that into BPE bilayers, then the three-capacitor model also fails to account for the magnitude of the changes in surface potential observed on monolayers.

The potential measured with an electrode much further away from the surface than the distance between the adsorbed ions is the macropotential of magnitude V_∞:

$$V_\infty = -\Delta(\Delta V) = \Delta V - \Delta V(T\phi B^-) = q^0/C_o^*, \tag{40}$$

where C_o^* is the capacitance of the outer region of the monolayer. When the ions are not uniformly smeared over the adsorption plane, the adsorption of ions will be determined by a micropotential of magnitude Φ:

$$q^0 = K^* \cdot F \cdot [T\phi B^-] \exp\{-e \cdot \Phi/kT\}, \tag{41}$$

where K^* is the adsorption coefficient of $T\phi B^-$ into the monolayer. The micropotential, Φ, will, in general, be lower in magnitude than the macropotential, V_∞. In our three-capacitor model, however, where we assume the adsorbed charges are smeared, both V_∞ and Φ are equal to V_o.

We present here the results of an analysis of the simplest possible discrete charge model relating Φ and V_∞ (Appendix E). We assume that the monolayer is a uniform slab of hydrocarbon, that the aqueous phase is a homogenous conductor, and that the adsorbed ions are fixed in a regular hexagonal or square lattice. With these assumptions we obtain the result that:

$$V_\infty = (K^* \cdot F/C_o^*) \cdot [T\phi B^-] \cdot \exp\{-\alpha \cdot e \cdot V_\infty^{3/2}/kT\}, \tag{42}$$

where α is a parameter which depends on the dielectric constant and the location of the plane of adsorbed charge in the monolayer. The solid curve in Fig. 6 represents the best fit of the data to Eq. 42, obtained with $\alpha = 0.93\ V^{-1/2}$ and $K^*/C_o^* = 4.9 \cdot 10^3 \text{Vcm}^3\text{C}^{-1}$. The two dashed curves indicate the sensitivity of the fit to the value of α.[10] The fit is probably fortuitous because the electrostatic model is oversimplified and because the adsorbed ions are assumed to be located in a fixed lattice, which overemphasizes discrete charge effects.

[10]The parameters α and K^*/C_o^* contain information about the properties of the outer region of the monolayer. From a knowledge of K^* and a combination of Eqs. E9 and E10 one can calculate δ^* and ϵ_r^*, where ϵ_r^* will be close to $\epsilon_r^{\text{outer}}$ of the monolayer (see Barlow and Macdonald, 1967, Fig. 25). If we assume that $K^* = K$ then one finds that $\epsilon_r^{\text{outer}} = \epsilon_r^* = 8$, and $\delta^* = 10$ Å).

f. DISCRETE CHARGE EFFECTS IN BILAYERS? Discrete charge effects may also be important in bilayers. Unfortunately, even an analysis such as the one we have just presented for monolayers is considerably more complicated for bilayers (e.g. Barlow and Macdonald, 1964, 1967) and to our knowledge has not been done.

The potential produced by the $T\phi B^-$ adsorbed in BPE bilayers, as deduced from probe measurements, changes by more than 2.3 kT/e per decade $[T\phi B^-]$ (see Fig. 5). This is analogous to an Esin-Markov coefficient greater than 2.3 kT/e and thus constitutes evidence for discrete charge effects in bilayers. This difference between Δv (the change in potential in the middle of the membrane) and Φ (the micropotential which determines the adsorption of $T\phi B^-$ into the wells) becomes more negative with increasing $[T\phi B^-]$ (see also Eq. E5).

$$d(\Delta v + \Phi)/d[T\phi B^-] < 0. \tag{43}$$

Since (see Eq. 41)

$$q^0 = F \cdot K \cdot [T\phi B^-] \cdot \exp\{-e\Phi/kT\}, \tag{44}$$

and

$$G(0,0) = g \cdot [T\phi B^-] \cdot \exp\{e\Delta v/kT\}, \tag{39}$$

then (see Andersen and Fuchs, 1975; and Szabo, 1976)

$$\tau = q^0/G(0,0) = (F \cdot K/g)\exp\{(-e/kT)(\Delta v + \Phi)\}. \tag{45}$$

The implication of Eqs. 43 and 45 is that τ will increase with increasing $[T\phi B^-]$. Such an increase is in fact observed (Fig. 3*c* and 4*c*).

The asymmetry of the anionic and cationic probe measurements also may be due to discrete charge effects. At any instant the potential along a plane in the middle of a bilayer is not uniform but rather exhibits peaks and valleys. If one assumes that the adsorbed anions are located in a fixed-square lattice on each side of the membrane, one can integrate the Boltzmann factors for an anionic and cationic probe and show that the decrement of anionic conductance and the enhancement of cationic conductance are not symmetrical.

4. Biological Implications

Adsorption of $T\phi B^-$ and other hydrophobic ions to the bilayer component of biological membranes will produce boundary potentials. These boundary potentials will affect the permeability of the membrane to hydrophobic ions or ion-carrier complexes. At low concentrations $T\phi B^-$ increases the uptake of hydrophobic cations into mitochondria (Bakeeva et al., 1970) and vesicles formed from bacteria (Altendorf et al., 1975). These observations are presumably due to $T\phi B^-$ increasing the permeability of the membrane to cations. Our conclusion that $T\phi B^-$ produces boundary potentials can thus provide a basis for the use of hydrophobic anions as "catalysts" for the uptake of cations across energy-transducing membranes.

The boundary potential produced by adsorption of $T\phi B^-$ into a biological membrane and the large electric field associated with this potential may also affect the properties of endogenous membrane carriers and transmembrane channels. $T\phi B^-$ and other hydrophobic ions may thus be used to perturb biological membranes.

The large adsorption coefficient of $T\phi B^-$ onto the membrane, however, contraindicates the use of this ion as a probe of the transmembrane potential of isolated cells and vesicles. The transmembrane potential, V_m, can be calculated from the ratio of the free concentrations of $T\phi B^-$ in the intracellular and extracellular fluids by using the Nernst equation:

$$V_m = (kT/e) \ln \{[T\phi B^-]_{in}/[T\phi B^-]_{out}\}$$

In practice one measures the total $T\phi B^-$ associated with the cell or vesicle. It can be shown that the ratio of the amount of $T\phi B^-$ adsorbed to the membrane to the amount of free $T\phi B^-$ in the cell will be small, less than 0.1, only when

$$(3 \cdot K/r) \cdot (\exp \{e \cdot \psi_{in}/kT\} + \exp \{e \cdot (\psi_{out} - V_m)/kT\}) < 0.1, \qquad (46)$$

where K is the adsorption coefficient into the membrane in the *absence* of any diffuse double layer potential, ψ_{in} and ψ_{out} are the diffuse double layer potentials of the interior and exterior membrane surface, respectively, and r is the radius of the vesicle or cell. If $V_m = \psi_{in} = \psi_{out} = -59$ mV and $K = 0.037$, r must be larger than $33 \cdot K \simeq 1$ cm!

The current transients associated with translocation of $T\phi B^-$ adsorbed to artificial bilayers may also be a useful model for the current transients associated with translocation of membrane-bound charges or dipoles in excitable membranes. Such currents have been inferred in photoreceptors (e.g. Hagins and Rüppel, 1971). Trissl et al. (1977) and Hong (1976) may be consulted for additional references and a discussion of similar currents in reconstituted and artificial systems. These currents have been observed in the transverse tubular system of skeletal muscle (Chandler et al., 1976; Adrian and Almers, 1976), and in unmyelinated (Armstrong and Bezanilla, 1975; Keynes and Rojas, 1976), and myelinated (Neumcke et al., 1976) nerve. Armstrong and Benzanilla (1975) reported that the gating currents for Na^+ channels recorded in giant axons of *Loligo pealei* have a nonexponential time-course, which within experimental error can be described as the sum of two exponentials (but see also Keynes and Rojas, 1976). This behavior is similar to that observed with $T\phi B^-$ at high absorbed charge densities where large changes in boundary potentials occur (see Fig. 6 in Andersen et al., 1977). It is not clear whether the biophysical basis for these observations is the same in artificial and biological membranes. It should be noted, however, that the local gating charge density around each Na^+ channel could be quite high (a few charges/10 nm^2), even though the average gating charge density of the squid axon is rather low due to the low density of Na^+ channels. The nonexponential gating current transients could, therefore, be due to boundary potentials produced by gating particles located in the interior of the membrane.

APPENDIX A

General Formalism for the Three-Capacitor Model

In the three-capacitor model both outer regions have been assigned the specific capacitance C_o. The outer capacitance, C_o, consists of two components in series: a capacitance C_{dl} due to the diffuse double layer and a capacitance C_b due to the outer region of the bilayer. Thus:

$$1/C_o = 1/C_{dl} + 1/C_b. \tag{A1}$$

This is analogous to Grahame's (1947, pp. 473–476) treatment relating the capacitances of the diffuse double layer and the Stern layer to the total capacitance of an electrode. A similar approach for bilayers has been discussed by Everitt and Haydon (1968) and de Levie (1977).

Several different experimental techniques have been used (e.g. McLaughlin, 1977) to confirm that the potential of the diffuse double layer, ψ, is related to the charge density by the Gouy equation:

$$\psi' = (2 \cdot kT/e) \operatorname{arcsinh} \{A \cdot (q_c - q^0)/\sqrt{c}\}, \tag{A2}$$

$$\psi'' = (2 \cdot kT/e) \operatorname{arcsinh} \{A \cdot (q_c + q^0)/\sqrt{c}\}, \tag{A3}$$

where

$$A = (8 \cdot N \cdot kT \cdot \epsilon_0 \cdot \epsilon_r^{aq})^{-1/2}, \tag{A4}$$

and c is the concentration of monovalent electrolyte in the bulk aqueous solution. These equations lead directly to expressions for the integral capacitances of the left and right diffuse double layers:

$$\frac{1}{C'_{dl}} = \frac{\psi'}{q_c - q^0} = \frac{2 \cdot kT}{e \cdot (q_c - q^0)} \cdot \operatorname{arcsinh} \left\{ \frac{\Delta \cdot (q_c - q^0)}{\sqrt{c}} \right\}. \tag{A5}$$

$$\frac{1}{C''_{dl}} = \frac{\psi''}{q_c + q^0} = \frac{2 \cdot kT}{e \cdot (q_c + q^0)} \cdot \operatorname{arcsinh} \left\{ \frac{A \cdot (q_c + q^0)}{\sqrt{c}} \right\}, \tag{A6}$$

and to expressions for the left and right outer capacitances:

$$\frac{1}{C'_o} = \frac{1}{C_b} + \frac{2 \cdot kT}{e \cdot (q_c - q^0)} \cdot \operatorname{arcsinh} \left\{ \frac{A \cdot (q_c - q^0)}{\sqrt{c}} \right\}, \tag{A7}$$

$$\frac{1}{C''_o} = \frac{1}{C_b} + \frac{2 \cdot kT}{e \cdot (q_c + q^0)} \cdot \operatorname{arcsinh} \left\{ \frac{A \cdot (q_c + q^0)}{\sqrt{c}} \right\}. \tag{A8}$$

When the argument of the arcsinh is sufficiently small:

$$A \cdot (q^0 + q_c)/\sqrt{c} < 0.5, \tag{A9}$$

a condition always satisfied in our experiments. Eqs. A5 and A6 simplify to:

$$1/C'_{dl} = 1/C''_{dl} = 1/C_{dl} = 2 \cdot A \cdot kT/e \cdot \sqrt{c} = 1/\kappa \cdot \epsilon_0 \cdot \epsilon_r^{aq}, \qquad \text{(A10)}$$

where $1/\kappa$ is the Debye length. It follows that

$$1/C'_o = 1/C''_o = 1/C_o = 1/C_b + 2 \cdot A \cdot kT/(e \cdot \sqrt{c}) = (\delta + 1/\kappa)/(\epsilon_0 \cdot \epsilon_r^{outer}), \qquad \text{(A11)}$$

where ϵ_r^{outer} is defined by:

$$\frac{\delta + 1/\kappa}{\epsilon_r^{outer}} = \frac{1}{\kappa \cdot \epsilon_r^{aq}} + \int_0^{\delta} \frac{1}{\epsilon_r} \, dx. \qquad \text{(A12)}$$

We can express the outer potential as the sum of the diffuse double-layer potential and the boundary potential within the membrane, Φ,

$$V'_o = \psi' + \phi' = (q_c - q^0)/C'_o = (q_c - q^0) \cdot (1/C'_{dl} + 1/C_b), \qquad \text{(A13)}$$

$$V''_o = \psi'' + \phi'' = (q_c + q^0)/C''_o = (q_c + q^0) \cdot (1/C''_{dl} + 1/C_b). \qquad \text{(A14)}$$

If the condition of Eq. A9 is not met, we must replace Eq. 7 by:

$$V_m = (q_c - q^0)/C'_o + (q_c + q^0 - q'')/C_i + (q_c + q^0)/C''_o \qquad \text{(A15)}$$

Inspection of Eqs. A5, A6, and A14 illustrate that in this case the values of C'_o and C''_0 are neither equal nor constant but depend upon $q^0 \pm q_c$, and thus depend upon the applied potential, V_m.

APPENDIX B

Derivation of Voltage-Clamp Equations

We assume that the voltage clamp is ideal. The derivative of Eq. 15 with respect to time gives

$$dV_m/dt = 0 = dq_c/dt + b \cdot d(q' - q^0)/dt, \qquad \text{(B1)}$$

or

$$i_c = dq_c/dt = -b dq'/dt, \qquad \text{(B2)}$$

where i_c is the current measured in the external circuit. (See also Ciani, 1976). Integration of Eq. B2 yields:

$$\Delta q_c = b \cdot (q^0 - q') = b \cdot (q'' - q^0) = q_c - V_m \cdot C_m. \qquad \text{(B3)}$$

When the intramembrane charge translocation is complete ($i_c = i = 0$) we can use the Boltzmann relation, Eq. 18, to express the distribution of charges between the two potential energy wells. From Eqs. 16 and B3 we obtain

$$V_i = b \cdot V_m - (1 - b) \cdot \Delta q_c/C_m, \qquad \text{(B4)}$$

and by combining Eqs. 3, 18, B3, and B4 we finally obtain

$$\frac{\Delta q_{c,max} + \Delta q_c}{\Delta q_{c,max} - \Delta q_c} = \exp\left\{\frac{e}{kT}\left[b \cdot V_m - \frac{(1 - b) \cdot \Delta q_c}{C_m}\right]\right\}, \qquad \text{(B5)}$$

where $\Delta q_{c,max} = b \cdot q^0$ is the upper limit of Δq_c when $V_m \to \infty$.

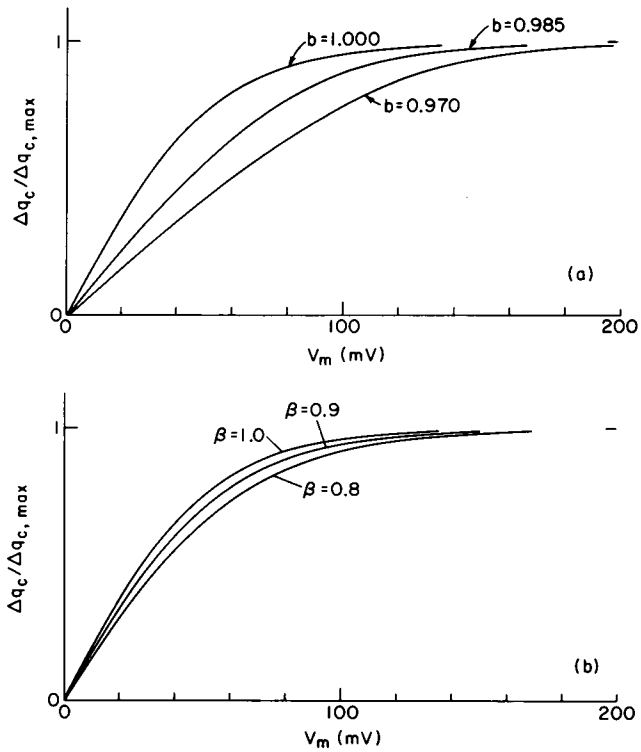

FIGURE 10 Theoretical predictions of charge translocation as a function of applied potential. (*a*) Predictions from the three-capacitor model, Eq. B5, with $\Delta q_{c,max} = 1\ \mu C/cm^2$ and the values of b indicated in the figure. (*b*) Predictions from a model that ignores boundary potentials, Eq. B6, with the indicated values of β.

Eq. B5 can be compared with Eq. 10 of Andersen and Fuchs (1975):

$$(\Delta q_{c,max} + \Delta q_c)/(\Delta q_{c,max} - \Delta q_c) = \exp\{e \cdot \beta \cdot V_m/kT\}. \quad \text{(B6)}$$

This equation neglects the modification of V_i by the charges adsorbed in the potential energy wells. In the limit of $q^0 \to 0$ we note that $\beta \to b$. The significance of the difference between Eqs. B5 and B6 is seen in Table I and in Fig. 10.

The three-capacitor model is not intended to be an equivalent circuit for the movement of $T\phi B^-$ within lipid bilayers. It is possible, however, to correlate our model parameters to an equivalent circuit capacitance, C_a as defined by de Levie et al. (1974*a*). If the membrane is stimulated with a sinusoidal potential of sufficiently low frequency so that the distribution of the adsorbed ions between the two potential energy wells is described by the Boltzmann relation, then Eq. B5 will still be valid. For values of $eV_i/(kT) \ll 1$, we can linearize Eq. 5 and with Eqs. 16 and 19 obtain:

$$\begin{aligned}(\Delta q_{c,max} + \Delta q_c)/(\Delta q_{c,max} - \Delta q_c) &= q''/q' = q''/(2 \cdot q^0 - q'') \\ &= 1 + (e/kT) \cdot (V_m - (1 - b) \cdot q_c/C_m). \quad \text{(B7)}\end{aligned}$$

We see that

$$d(q''/q')/dV_m = [2 \cdot q^0/(2 \cdot q^0 - q'')^2] \cdot dq''/dV_m. \quad \text{(B8)}$$

Since there will be relatively little charge translocation for a small voltage perturbation:

$$q'' \simeq q^0, \quad \text{(B9)}$$

and, therefore

$$\frac{d(q''/q')}{dV_m} = \frac{2}{q^0} \cdot \frac{dq''}{dV_m} = \frac{e}{kT} \cdot \left(1 - \frac{(1-b)}{C_m} \cdot \frac{dq_c}{dV_m}\right). \quad \text{(B10)}$$

From Eq. B3 we obtain:

$$dq_c/dV_m = b \cdot dq''/dV_m + C_m, \quad \text{(B11)}$$

which, combined with Eq. B10, gives:

$$dq_c/dV_m = C_m^* = \frac{C_m + (e/kT) \cdot q^0 \cdot b/2}{1 + (e/kT) \cdot (1-b) \cdot b \cdot q^0/(2C_m)}, \quad \text{(B12)}$$

where C_m^* is the measured capacitance.

In our three-capacitor model, we assume that charge movement across the outer regions of the membrane is negligible, which is equivalent to assuming an infinite Warburg impedance. The adsorption capacitance, as defined by de Levie et al. (1974*a*), is our model:

$$C_a = C_m^* - C_m = \frac{(e/kT) \cdot (q/2) \cdot b^2}{1 + (e/kT) \cdot (1-b) \cdot b \cdot q^0/(2C_m)}, \quad \text{(B13)}$$

or with Eq. 22

$$C_a = \frac{(e/kT) \cdot b \cdot \Delta q_{c,\max}/2}{1 + (e/kT) \cdot (1-b) \cdot \Delta q_{c,\max}/(2C_m)}. \quad \text{(B14)}$$

APPENDIX C

Derivation of Charge-Pulse Equations

We assume that the charge is injected instantaneously and that after injection:

$$dq_c/dt = 0. \quad \text{(C1)}$$

From Eq. 15:

$$V_m(\infty) = [q_c + b \cdot (q' - q^0)]/C_m. \quad \text{(C2)}$$

From Eqs. C1, C2, and 23

$$\Delta V_m = V_m(0) - V_m(\infty) = b \cdot (q'' - q^0)/C_m = b \cdot (q^0 - q')/C_m. \quad \text{(C3)}$$

Combining Eqs. 13 and 15, we obtain:

$$V_i = V_m - (1-b) \cdot q_c/C_m. \quad \text{(C4)}$$

Since we are interested in the value of V_m after the charge has been translocated and a Boltz-

mann distribution between the wells has been established, we write:

$$V_i(\infty) = V_m(\infty) - (1 - b) \cdot q_c/C_m. \tag{C5}$$

We combine Eq. C5 and Eqs. 23 and C3 to give:

$$V_i(\infty) = V_m(\infty) - (1 - b) \cdot V_m(0) = b \cdot V_m(0) - \Delta V_m. \tag{C6}$$

From the Boltzmann relation

$$q''/q' = \exp\{e \cdot V_i/kT\}. \tag{C7}$$

If $V_i(\infty)$ is large enough to effect translocation of all the ions from one well to the other, $q' \rightarrow 0$ and $q'' \rightarrow 2q^0$. The maximum value of ΔV_m, $\Delta V_{m,\max}$, may then be deduced directly from Eq. C3:

$$\Delta V_{m,\max} = b \cdot q^0/C_m. \tag{C8}$$

Combining Eqs. C3, C6, C7, and C8 then gives:

$$(\Delta V_{m,\max} + \Delta V_m)/(\Delta V_{m,\max} - \Delta V_m) = \exp\{(e/kT)(b \cdot V_m(0) - \Delta V_m)\}. \tag{C9}$$

APPENDIX D

Difference in Dipole Potential between BPE and GMO Bilayers

The overall difference in interfacial dipole potentials between BPE and GMO membranes may be estimated by measuring the conductances due to cations and anions. Table II summarizes our data using K^+-nonactin, the HA_2^- complex of the weak acid DTFB, and $T\phi B^-$ as probes. Qualitatively, we find that anion conductances are higher in BPE membranes than in GMO membranes, while cation conductances are higher in the latter membranes. Quantitatively, we find that the increase in cation conductance (going from BPE to GMO) is almost one order of magnitude larger than the decrease in anion conductance. Similar discrepancies have been observed between BPE and glyceroldioleate-decane membranes, with K^+-nonactin and I_2/I^- as probes (Szabo et al., 1972). The interpretation of conductance changes is ambiguous when different probes exhibit different relative conductance changes. It becomes impossible to exclude some specific interactions (i.e. nonelectrostatic, nonmobility) between the probe ion and the membrane matrix. If one assumes such specific interactions to be negligible, one can use the above results to calculate the relative permeability changes (due, for example, to a difference in membrane thickness, fluidity or dielectric constant), as well as the difference in interfacial dipole potentials. The membrane conductance can be written as (see also Szabo, 1976):

TABLE II

RELATIVE CHANGES IN CONDUCTANCE, DIPOLE POTENTIAL, AND PERMEABILITY IN GMO AND BPE MEMBRANES

	$T\phi B^-$	Nonactin-K^+	$DTFB^-$
Observed			
G_{BPE}/G_{GMO}	66	0.0015	25
Estimated			
$\Delta V_D, mV$	137	124	
P_{BPE}/P_{GMO}	0.32	0.19	

$$G(0,0) = (e^2F/kT) \cdot P \cdot [T\phi B^-] \cdot \exp\{e \cdot V_D/kT\}, \quad (D1)$$

where P is a permeability coefficient and V_D is the interfacial dipole potential. We can write similar expressions for each current carrier in both BPE and GMo membranes, and compare the relative conductance changes of nonactin-K^+ with those for $T\phi B^-$ or for DTFB. We make the assumption that:

$$P_{GMO}{}^+/P_{GMO}{}^- = P_{BPE}{}^+/P_{BPE}{}^- \quad (D2)$$

where $P_{GMO}{}^+$ is the permeability coefficient of GMO bilayers for the positive probe, as defined in Eq. 1, etc. The difference in dipole potential between BPE and GMO bilayers, ΔV_D, can be expressed as:

$$\Delta V_D = (kT/e) \ln\{(G_{GMO}{}^+/G_{BPE}{}^+) \cdot (G_{BPE}{}^-/G_{GMO}{}^-)\}^{1/2}, \quad (D3)$$

and the permeability ratio can be expressed as:

$$P_{GMO}/P_{BPE} = \{(G_{GMO}{}^+/G_{BPE}{}^+) \cdot (G_{GMO}{}^-/G_{BPE}{}^-)\}^{1/2}. \quad (D4)$$

The results of these comparisons are given in Table II. We find, in agreement with earlier workers (Hladky, 1974), that the interfacial dipole potential is more positive in BPE than in GMO membranes. The value we obtain in this manner, $\Delta V_D \simeq 130$ mV, agrees with the difference in the surface potentials of hydrocarbon containing BPE and GMO monolayers (O. Andersen, unpublished).

APPENDIX E

Discrete charge phenomena

THE ESIN-MARKOV COEFFICIENT The combination of Eq. 32 and 33 yields:

$$d V_o/d \ln [T\phi B^-] = V_o - (e \cdot V_o/kT) \cdot d V_o/d \ln [T\phi B^-]),$$

or

$$d V_o/d \log [T\phi B^-] = (2.303 \cdot kT/e) \cdot V_o/(kT/e + V_o) < 2.303 \cdot kT/e, \quad (E2)$$

(recall that $V_o > 0$). Thus, within the framework of the three-capacitor model the Esin-Markov coefficient, $dV_o/d \log [T\phi B^-]$ must be less than 59 mV at room temperature.

In general, we can combine Eqs. 40 and 41 to obtain:

$$d V_\infty/d \log [T\phi B^-] = (2.303 \cdot kT/e) \cdot V_\infty/(kT/e + V_\infty \cdot d\Phi/d V_\infty), \quad (E3)$$

where V_∞ is a macropotential and Φ is the micropotential. An Esin-Markov coefficient larger than 2.303 kT/e can, therefore, only occur if

$$d\Phi/d V_\infty < 1, \quad (E4)$$

or

$$d\Phi/d[T\phi B^-] < d V_\infty/d[T\phi B^-] \quad (E5)$$

THE HEXAGONAL LATTICE MODEL OF $T\phi B^-$ ADSORPTION INTO MONOLAYERS The monolayer is assumed to be a uniform slab of hydrocarbon with a dielectric constant ϵ_r^*, the aqueous solution a perfect conductor, and the interface a mathematically planar boundary. We neglect the presence of the hydrocarbon-air interface. We also neglect the thermal movement of the adsorbed charges and assume that a square or hexagonal array of charges is located a distance δ^* from the monolayer-solution interface. We ignore any potential energy contri-

butions due to rearrangement of the lattice when ions adsorb into the monolayer. Each adsorbed charge will induce a polarization charge (of opposite sign) at the interface, and the electric field variation in the monolayer around each adsorbed charge will be identical to that of a dipole in a macroscopic medium of dielectric constant ϵ_r^* (see, for example, Bleaney and Bleaney, 1965). The micropotential, Φ, which determines the adsorption of charges into the bilayer, can be calculated if we can calculate the mutual potential energy, U, per unit area (square centimeters) of an infinite planar lattice of dipoles,

$$U(n) = \tfrac{1}{2} \cdot n \cdot e \cdot 2 \cdot \phi, \tag{E6}$$

where n is the number of charges per square centimeters. An expression for $U(n)$ was derived by Topping (1927), assuming ideal point dipoles:

$$U(n) = \tfrac{1}{2} \cdot n^{5/2} \cdot \mu^2 \cdot \kappa_T / (4 \cdot \pi \cdot \epsilon_r^* \cdot \epsilon_0). \tag{E7}$$

where μ is the dipole moment in coulomb-centimeters and κ_T is a constant having the value 9.03 for a square lattice and 8.89 for a hexagonal lattice. By combining Eqs. E6 and E7 we obtain:

$$\Phi = n^{3/2} \cdot (2 \cdot \delta^*)^2 \cdot e \cdot \kappa_T / (8 \cdot \pi \cdot \epsilon_r^* \cdot \epsilon_0). \tag{E7}$$

We also have that:

$$V_\infty = n \cdot e \cdot \delta^* / (\epsilon_0 \cdot \epsilon_r^*) = q^0 / C_o^* \tag{E9}$$

By eliminating n between Eqs. E8 and E9 we obtain:

$$\Phi = [\kappa_T / (2\pi)] \cdot \sqrt{\epsilon_0 - \epsilon_r^* \cdot \delta^* / e} \cdot V_\infty^{3/2} = \alpha V_\infty^{3/2} \tag{E10}$$

where

$$\alpha = [\kappa_T / (2\pi)] \cdot \sqrt{\epsilon_0 \cdot \epsilon_r^* \cdot \delta^* / e} \tag{E11}$$

From the definition of the micropotential we have:

$$q^0 = K^* \cdot F \cdot [\mathrm{T}\phi\mathrm{B}^-] \cdot \exp\{-e\Phi / kT\} \tag{E12}$$

where K^* is the adsorption coefficient of $\mathrm{T}\phi\mathrm{B}^-$ in the monolayer so:

$$V_\infty = (K^* \cdot F / C_o^*) \cdot [\mathrm{T}\phi\mathrm{B}^-] \cdot \exp\{-e \cdot \alpha \cdot V_\infty^{3/2} / kT\}, \tag{E13}$$

and the Esin-Markov coefficient is:

$$\mathrm{d}V_\infty / \mathrm{d} \log [\mathrm{T}\phi\mathrm{B}^-] = (2.303 \cdot kT/e) \cdot V_\infty / (kT/e + \tfrac{3}{2} \cdot \alpha \cdot V_\infty^{3/2}) \tag{E14}$$

from which we can determine α from a plot of V_∞ vs. $\log [\mathrm{T}\phi\mathrm{B}^-]$.

We thank Dr. G. Colacicco of Albert Einstein College of Medicine for the use of his monolayer equipment and for advice on the surface potential experiments. We acknowledge the valuable comments of S. Hladky, G. Szabo, and R.Y. Tsien.

Dr. Andersen thanks C. Martin for excellent technical assistance with some of the experiments.

Dr. Andersen was a New York Heart Association Senior Investigator and acknowledges support from National Institutes of Health grant GM 21342. Dr. McLaughlin acknowledges support from National Science Foundation grant PCM 76-04363. Dr. Feldberg acknowledges support from the Division of Basic Energy Sciences, U.S. Department of Energy, Washington, D.C., under contract EY-76-C-02-0016.

Received for publication 29 June 1977 and in revised form 19 September 1977.

REFERENCES

ADRIAN, R. H., and W. ALMERS. 1976. Charge movement in the membrane of striated muscle. *J. Physiol. (Lond.).* **254**:339.

ALTENDORF, K., H. HIRATA, and F. M. HAROLD. 1975. Accumulation of lipid-soluble ions and of rubidium as indicators of the electrical potential in membrane vesicles of *Escherichia coli*. *J. Biol. Chem.* **250**: 1405.

ANDERSEN, O. S., and M. FUCHS. 1975. Potential energy barriers to ion transport within lipid bilayers. Studies with tetraphenylborate. *Biophys. J.* **15**:795.

ANDERSEN, O. S., A. FINKELSTEIN, I. KATZ, and A. CASS. 1976. The effect of phloretin on the permeability of thin lipid membranes. *J. Gen. Physiol.* **67**:749.

ANDERSEN, O., S. FELDBERG, H. NAKADOMARI, S. LEVY, and S. MCLAUGHLIN. 1977. Electrostatic potentials associated with the absorption of tetraphenylborate into lipid bilayer membranes. *In* Ion Transport across Membranes. The Proceedings of a Joint US-USSR Conference. D. Tosteson, Yu. A. Ovchinnikov, and R. Latorre, editors. Raven Press, New York: 327.

ARMSTRONG, C. M., and F. BEZANILLA. 1975. Currents associated with the ionic gating structure in nerve membrane. *Ann. N.Y. Acad. Sci.* **264**:265.

AVEYARD, R., and D. A. HAYDON. 1973. An Introduction to the Principles of Surface Chemistry. Cambridge University Press, London, England.

BABAKOV, A. V., I. V. MYAGKOV, P. S. SOTNIKOV, and P. TEREKHOV. 1972. Study of the surface potential of phospholipid monolayers at the interface air-water and physico chemical properties of phospholipid membranes. *Biofizika.* **17**:347.

BAKEEVA, L. E., L. L. GRINIUS, A. A. JASAITIS, V. V. KULIENE, D. O. LEVITSKY, E. A. LIBERMAN, I. I. SEVERINA, and V. P. SKULACHEV. 1970. Conversion of biomembrane-produced energy into electric form. II. Intact mitochondria. *Biochim. Biophys. Acta.* **216**:13.

BANGHAM, A. D., M. W. HILL, and N. G. A. MILLER. 1974. Preparation and use of liposomes as models of biological membranes. *Meth. Membrane Biol.* **1**:1.

BARLOW, C. A., and J. R. MACDONALD. 1964. Discreteness-of-charge adsorption micro-potentials. I. Infinite imaging. *J. Chem. Phys.* **40**:1535.

BARLOW, C. A., and J. R. MACDONALD. 1967. Theory of discreteness of charge effects in the electrolyte compact double layer. *Adv. Electrochem. Electrochem. Eng.* **6**:1.

BENZ, R., P. LÄUGER, and K. JANKO. 1976. Transport kinetics of hydrophobic ions in lipid bilayer membranes: charge-pulse relaxation studies. *Biochim. Biophys. Acta.* **455**:701.

BENZ, R., and P. LÄUGER. 1977. Transport kinetics of dipicrylamine through lipid bilayer membranes: effects of membrane structure. *Biochim. Biophys. Acta.* **468**:245.

BLEANEY, B. I., and B. BLEANEY. 1965. Electricity and Magnetism. 2nd edition. Oxford University Press, London.

BRUNER, L. J. 1975. The interaction of hydrophobic ions with lipid bilayer membranes. *J. Membrane Biol.* **22**:125.

CHANDLER, W. K., R. F. RAKOWSKI, and M. F. SCHNEIDER. 1976. A nonlinear voltage dependent charge movement in frog skelectal muscle. *J. Physiol. (Lond.).* **254**:245.

CIANI, S. 1976. Influence of molecular variations of ionophore and lipid on the selective ion permeability of membranes. II. A theoretical model. *J. Membrane Biol.* **30**:45.

DELEVIE, R., N. G. SEIDAH, and H. MOREIRA. 1974*a*. Transport of ions of one kind through thin membranes. IV. Admittance for membrane-soluble ions. *J. Membrane Biol.* **16**:17.

DELEVIE, R., N. G. SEIDAH, and D. LARKIN. 1974*b*. Tetraphenylborate adsorption onto an artificial ultrathin membrane. *J. Electroanal. Chem. Interfacial Electrochem.* **49**:153.

DELEVIE, R., and D. VUKADIN. 1975. Dipicrylamine transport across an ultrathin phosphatidylethanolamine membrane. *J. Electroanal. Chem. Interfacial Electrochem.* **62**:95.

DELEVIE, R. 1977. Ionic adsorption and the conductance of ultrathin lipid membranes. *J. Electroanal. Chem. Interfacial. Electrochem.* **82**:361.

EDSALL, J. T., and J. WYMAN. 1958. Some general aspects of molecular interactions. *In* Biophysical Chemistry, Vol. I. Thermodynamics, Electrostatics, and the Biological Significance of the Properties of Matter. Academic Press, Inc., New York. 591.

EVERITT, C. T., and D. A. HAYDON. 1968. Electrical capacitance of a lipid membrane separating two aqueous phases. *J. Theor. Biol.* **18**:371.

FELDBERG, S. W., and G. KISSEL. 1975. Charge pulse studies of transport phenomena in bilayer membranes. I. Steady state measurements of actin-and valinomycin-mediated transport in glycerol monooleate bilayers. *J. Membrane Biol.* **20**:269.

FELDBERG, S. W., and H. NAKADOMARI. 1977. Charge pulse studies of transport phenomena in bilayer membranes: II. Detailed theory of steady-state behavior and application to valinomycin-mediated potassium transport. *J. Membrane Biol.* **31**:81.

FELDBERG, S. W., and A. B. DELGADO. 1978. Inner voltage clamping. A method for studying interactions among hydrophobic ions in a lipid bilayer membrane. *Biophys. J.* **21**:71.

GAVACH, C., and R. SANDEAUX. 1975. Non-mediated zero voltage conductance of hydrophobic ions through bilayer lipid membranes. *Biochim. Biophys. Acta.* **413**:33.

GINSBURG, H., and G. STARK. 1976. Facilitated transport of Di and trinitrophenylate ions across lipid membranes by valinomycin and nonactin. *Biochim. Biophys. Acta.* **455**:685.

GRAHAME, D. C. 1947. The electrical double layer and the theory of electrocapillarity. *Chem. Rev.* **41**:441.

GRAHAME, D. C. 1958. Discreteness-of-charge-effects in the inner region of the electrical double layer. *Z. Elektrochem.*, **62**:264.

GRIGOR'EV, P. A., L. N. YERMISHKIN, and V. S. MARKIN. 1972. Direct passage of ions across lipid membranes. II. Experimental. *Biofizika.* **17**:788.

HAGINS, W. A., and H. RÜPPEL. 1971. Fast photoelectric effects that the properties of vertebrate photoreceptors as electric cables. *Fed. Proc.* **30**:64.

HAYDON, D. A., and S. B. HLADKY. 1972. Ion transport across thin lipid membranes: a critical discussion of mechanisms in selected systems. *Q. Rev. Biophys.* **5**:187.

HAYDON, D. A., and V. B. MYERS. 1973. Surface charge, surface dipoles and membrane conductance. *Biochim. Biophys. Acta.* **307**:429.

HINKLE, P. 1970. A model system for mitochondrial ion transport and respiratory control. *Biochem. Biophys. Res. Commun.* **41**:1375.

HLADKY, S. B., and D. A. HAYDON. 1973. Membrane conductance and surface potential. *Biochim. Biophys. Acta.* **318**:464.

HLADKY, S. B. 1974. The energy barriers to ion transport by nonactin across thin lipid membranes. *Biochim. Biophys. Acta.* **352**:71.

HONG, F. 1976. Charge transfer across pigmented bilayer lipid membrane and its interfaces. *Photochem. Photobiol.* **24**:155.

KETTERER, B., B. NEUMCKE, and P. LÄUGER. 1971. Transport mechanism of hydrophobic ions through lipid bilayer membranes. *J. Membrane Biol.* **5**:225.

KEYNES, R. D., and E. ROJAS. 1976. The temporal and steady state relationships between activation of the sodium conductance and movement of the gating particle in the squid giant axon. *J. Physiol. (Lond.).* **255**:157.

LÄUGER, P., and B. NEUMCKE. 1973. Theoretical analysis of ion conductance in lipid bilayer membranes. *In* Membranes. Vol. 2. G. Eisenman, editor. Marcel Dekker, Inc., New York: 1.

LE BLANC, O. H., JR. 1969. Tetraphenylborate conductance through lipid bilayer membranes. *Biochim. Biophys. Acta.* **193**:300.

LIBERMAN, Y. A., and D. M. MARGULIS. 1974. Permeability of spatial and boundary charges of bimolecular phospholipid membranes. I. Distribution coefficient. *Biofizika.* **19**:450.

LIBERMAN, Y. A., and V. P. TOPALY. 1968. Transfer of ions across bimolecular membranes and classification of uncouplers of oxidative phosphorylation. *Biofizika.* **13**:1025.

LIBERMAN, Y. A., and V. P. TOPALY. 1969. Permeability of bimolecular phospholipid membranes for lipid soluble ions. *Biofizika.* **14**:452.

MACDONALD, R. C., and A. D. BANGHAM. 1972. Comparison of double layer potentials in lipid monolayers and lipid bilayer membranes. *J. Membrane Biol.* **7**:29.

MCLAUGHLIN, S. G. A., G. SZABO, G. EISENMAN, and S. M. CIANI. 1970. Surface charge and the conductance of phospholipid membranes. *Proc. Natl. Acad. Sci.* U.S.A. **67**:1268.

MCLAUGHLIN, S. G., G. SZABO, and G. EISENMAN. 1971. Divalent ions and the surface potential of charged phospholipid membranes. *J. Gen. Physiol.* **58**:667.

MCLAUGHLIN, S. G. A. 1973. Salicylates and phospholipid bilayer membranes. *Nature (Lond.).* **243**:234.

MCLAUGHLIN, S. 1975. Local anesthetics and electrical properties of phospholipid bilayer membranes. *In* Molecular Mechanism of Anesthesia. B. R. Fink, editor. *Progress in Anesthesiology.* Volume 1, Raven Press, Inc., New York: 193.

McLAUGHLIN, S., and H. HARARY. 1976. The hydrophobic adsorption of charged molecules to bilayer membranes. A test of the applicability of the Stern equation. *Biochemistry.* **15**:1941.

McLAUGHLIN, S. 1977. Electrostatic potentials at membrane-solution interfaces. *Curr. Top. Membranes Transp.* **9**:71.

MARKIN, V. S., P. A. GRIGOR'EV, and L. N. YERMISHKIN. 1971. Forward passage of ions across lipid membranes. I. Mathematical model. *Biofizika.* **16**:1011.

MUELLER, P., D. O. RUDIN, H. TI TIEN, and W. C. WESCOTT. 1963. Methods for the formation of single bimolecular lipid membranes in aqueous solution. *J. Phys. Chem.* **67**:534.

MUELLER, P., and D. O. RUDIN. 1967. Development of K^+-Na^+ discrimination in experimental bimolecular lipid membranes by macrocyclic antibiotics. *Biochem. Biophys. Res. Commun.* **26**:398.

MUELLER, P., and D. O. RUDIN. 1969. Translocators in bimolecular lipid membranes: their role in dissipative and conservative bioenergy transductions. *Curr. Top. Bioenerg.* **3**:157.

NEUMCKE, B., W. NONNER, and R. STÄMPFLI. 1976. Asymmetrical displacement current and its relation with the activation of sodium current in the membrane of frog myelinated nerve. *Pflügers Arch. Eur. J. Physiol.* **363**:193.

OVERBEEK, J. TH.G., and P. H. WIERSEMA. 1967. The interpretation of electrophoretic mobilities. *In* Electrophoresis. M. Bier, editor. Volume 2. 1.

PALTAUF, F., H. HAUSER, and M. C. PHILLIPS. 1971. Monolayer characteristics of some 1,2-diacyl, 1-alkyl-2-acyl and 1,2-dialkyl phospholipids at the air-water interface. *Biochim. Biophys. Acta.* **249**:539.

SARGENT, D. F. 1976. An apparatus for the measurement of very small membrane relaxation currents. *Anal. Biochem.* **70**:100.

SHAW, D. J. 1970. Introduction to colloid and surface chemistry. Butterworth, London. 236.

SZABO, G., G. EISENMAN, and S. CIANI. 1969. The effects of the macrotetralide actin antibiotics on the electrical properties of phospholipid bilayer membranes. *J. Membr. Biol.* **1**:346.

SZABO, G. 1976. The influence of dipole potentials on the magnitude and the kinetics of ion transport in lipid bilayer membranes. *In* Extreme Environment: Mechanisms of Microbial Adaptation. G. R. Heinrich, editor. Academic Press, Inc., New York. 321.

SZABO, G., G. EISENMAN, S. G. A. McLAUGHLIN, and S. KRASNE. 1972. Ionic probes of membrane structures. *Ann. N. Y. Acad. Sci.* **195**:273.

TOPPING, J. 1927. On the mutual potential energy of a plane network of doublets. *Proc. R. Soc. Lond. Ser. A. Math. Phys. Sci.* **114**:67.

TRISSL, H. W., A. DARSZON, and M. MONTAL. 1977. Rhodopsin in model membranes: charge displacements in interfacial layers. *Proc. Natl. Acad. Sci. U.S.A.* **74**:207.

WANG, C. C., and L. J. BRUNER. 1977. Evidence for dielectric saturation of the aqueous phases adjacent to charged bilayer membranes. *Biophys. J.* **17**:131*a*. (Abstr.).

WULF, J., R. BENZ, and W. G. POHL. 1977. Properties of bilayer membranes in the presence of dipicrylamine. A comparative study by optical absorption and electrical relaxation measurements. *Biochim. Biophys. Acta.* **465**:429.